ADVANCED HEALTHCARE MATERIALS
www.advhealthmat.de

A Hydrogen-Bonded Extracellular Matrix-Mimicking Bactericidal Hydrogel with Radical Scavenging and Hemostatic Function for pH-Responsive Wound Healing Acceleration

Zainab Ahmadian, Alexandra Correia, Masoud Hasany, Patrícia Figueiredo, Faramarz Dobakhti, Mohammad Reza Eskandari, Seyed Hojjat Hosseini, Ramin Abiri, Shiva Khorshid, Jouni Hirvonen, Hélder A. Santos, and Mohammad-Ali Shahbazi**

Generation of reactive oxygen species, delayed blood clotting, prolonged inflammation, bacterial infection, and slow cell proliferation are the main challenges of effective wound repair. Herein, a multifunctional extracellular matrix-mimicking hydrogel is fabricated through abundant hydrogen bonding among the functional groups of gelatin and tannic acid (TA) as a green chemistry approach. The hydrogel shows adjustable physicochemical properties by altering the concentration of TA and it represents high safety features both in vitro and in vivo on fibroblasts, red blood cells, and mice organs. In addition to the merit of facile encapsulation of cell proliferation-inducing hydrophilic drugs, accelerated healing of skin injury is obtained through pH-dependent release of TA and its multifaceted mechanisms as an antibacterial, antioxidant, hemostatic, and anti-inflammatory moiety. The developed gelatin-TA (GelTA) hydrogel also shows an outstanding effect on the formation of extracellular matrix and wound closure in vivo via offered cell adhesion sites in the backbone of gelatin that provide increased re-epithelialization and better collagen deposition. These results suggest that the multifunctional GelTA hydrogel is a promising candidate for the clinical treatment of full-thickness wounds and further development of wound dressing materials that releases active agents in the neutral or slightly basic environment of infected nonhealing wounds.

1. Introduction

Skin has an important role in the maintenance of body homeostasis by protecting it from many noxious substances that can cause different diseases and bring serious discomfort and health hazard to human's normal life.[1,2] In recent years, the therapeutic impedance of wounds has become a major clinical challenge that has caused tremendous economic burden worldwide.[3,4] Owing to the complexity of the wound repair by itself and in the case of severe wound occurrence, ideal multifunctional healing strategies are needed to affect all four stages of the wound healing process, including hemostasis, inflammation, proliferation, and remodeling.[5] While various biomaterial-based systems have been developed for wound healing through biological alteration of the above-mentioned stages,[6–9] the introduction of cheap antibacterial and anti-bleeding hydrogels that display desirable impacts on all stages of wound healing process is still an unmet

Z. Ahmadian, A. Correia, Dr. P. Figueiredo, Prof. J. Hirvonen, Prof. H. A. Santos, Dr. M.-A. Shahbazi
Drug Research Program
Division of Pharmaceutical Chemistry and Technology
Faculty of Pharmacy
University of Helsinki
Helsinki FI-00014, Finland
E-mail: helder.santos@helsinki.fi; m.a.shahbazi@helsinki.fi

Z. Ahmadian, Dr. F. Dobakhti
Department of Pharmaceutics
School of Pharmacy
Zanjan University of Medical Science
Zanjan 45139-56184, Iran

Dr. M. Hasany
Department of Chemical and Petroleum Engineering
Sharif University of Technology
Azadi Avenue Tehran, Iran

Dr. M. R. Eskandari
Department of Pharmacology and Toxicology
School of Pharmacy
Zanjan University of Medical Science
Zanjan 45139-56184, Iran

The ORCID identification number(s) for the author(s) of this article can be found under https://doi.org/10.1002/adhm.202001122

DOI: 10.1002/adhm.202001122

essential. For example, in addition to anti-hemorrhage and antibacterial effect, a preferred multifunctional formulation for wound healing should inhibit the overproduction of free radicals and long-term secretion of pro-inflammatory cytokines in the wound tissue.[3,4] In addition, facile fabrication and low cost must be taken into account while designing a novel material for wound healing.

Natural hydrogels, as affordable hydrophilic polymeric 3D configurations, are attractive candidates for wound healing acceleration because of their structural similarity to the extracellular matrix (ECM), adjustable physicomechanical properties, wound protection from microbial invasion, and biodegradability.[3,10–13] Among natural polymers, collagen is highly suggested for hydrogel-mediated tissue engineering, because of its desirable effect on cell adhesion, migration, and proliferation.[14] Nevertheless, it has very high price, and therefore, gelatin can be considered as an alternative due to its lack of immunogenicity and low cost, while representing many unique properties of the collagen, such as high biocompatibility, no skin irritation, high absorption of tissue exudates, desirable cell attachment, capability to maintain a moist wound environment, and allowing oxygen permeation into the damaged tissue.[15–17] In addition, gelatin provides arginine-glycine-aspartic acid (RGD) peptide sequence that imparts favorable cell adhesion and higher hemostatic capacity to hydrogels made by this polymer.[13,18] Moreover, the target sequences of matrix metalloproteinase (MMP) are available in the structure of gelatin for beneficial cell remodeling.[19] These are the main reasons for the broad investigation of gelatin-based hydrogels for wound healing in recent years. However, there is still no ideal gelatin-based hydrogel in the market to support all four phases of wound repair by combined hemostatic, anti-inflammatory and antibacterial, cell proliferative and regenerative functions. Poor mechanical properties and sensitivity to water are the main limitations for the bench to bedside translation of gelatin-based hydrogels.[20,21]

To overcome these limitations, chemically active synthetic crosslinkers could improve the mechanical properties and stability of gelatin hydrogels.[20] Nevertheless, they endow hydrogels with toxicity and higher cost,[22] which are insuperable obstacles for their clinical translation. Instead, physical entanglement by naturally occurring polymers or materials can be a better option since they are usually cost-effective and biologically friendly, while the fabrication process is rapid, simple, and scalable.[23,24] For example, tannic acid (TA), a plant-derived polyphenol, has been recently attracted high attention for one-pot physical synthesis of hydrogels by numerous hydrogen bonding with other polymers, such as polyvinyl alcohol (PVA),[25] polyvinylpyrrolidone (PVP),[26] carboxylated agarose,[27] and DNA.[28] TA can render intrinsic anti-inflammatory, antioxidant, and antibacterial properties to the hydrogels.[27,29] Since severe cytotoxicity and detrimental consequences of drug resistance have limited the long-term application of antibiotics in chronic skin ulcers, using TA in advanced multifunctional wound dressing can be considered as a non-antibiotic therapeutic approach. Moreover, via interaction with blood proteins, TA can improve the hemostatic effect of the hydrogels.[30]

In this study, TA was introduced into a gelatin solution for one-pot fabrication of multifunctional gelatin-TA (GelTA) hydrogel through hydrogen bonding. GelTA can act as a drug delivery vehicle due to its highly porous structure. Therefore, during the synthesis procedure, allantoin (Alla) was mixed with the gelatin solution to prepare GelTA-Alla hydrogel for wound healing. Alla, which is mainly extracted from the root of the comfrey plant,[31] is a nonirritating compound with the ability of stimulating skin regrowth by reducing inflammation, triggering cell migration and proliferation, inducing keratolytic activity, promoting collagen formation, and also, reducing itching and pain at the site of skin injury.[32,33] In general, all components of the GelTA-Alla hydrogel were chosen to offer a multifaceted framework that has various mechanisms of actions as shown in **Scheme 1**, achieved by the combined effects of gelatin, TA, and Alla in the wound site.

2. Results and Discussion

2.1. Hydrogel Fabrication and Characterization

In the field of tissue engineering, hydrogels are rapidly under progress as 3D hydrophilic polymeric matrices that can be made from a wide range of natural and synthetic polymers for versatile functions through the control of cellular behavior and mimicking the native microenvironments of tissues.[34] Due to the inability of imitating ECM, lack of cell-recognition signals, high risk of eliciting immune reactions, and high price in many cases, synthetic materials are less of interest as compared to natural polymers for the restoration of damaged tissues. In this study, the green GelTA hydrogel was developed by means of hydrogen bonding between porcine skin gelatin (PSG), as a natural biopolymer,[35] and TA, which is a plant-derived polyphenolic biomolecule (**Figure 1**a).[27,36] By introducing TA solution into gelatin solution and simple mixing, the hydrogel was formed very rapidly via the creation of abundant hydrogen bonds between hydroxyl groups of TA as hydrogen donors and carboxyl and amine groups of gelatin as hydrogen acceptors (Figure 1b). In fact, physical entanglement of the polymer chains with TA through hydrogen bonding, which is one of the safest crosslinking methods for hydrogel formation, was occurred during the gelation

Dr. S. H. Hosseini
Department of Pharmacology
School of Medicine
Zanjan University of Medical Sciences
Zanjan 45139-56111, Iran
Dr. R. Abiri
Department of Microbiology
School of Medicine
Kermanshah University of Medical Sciences
Kermanshah 67148-69914, Iran
S. Khorshid, Dr. M.-A. Shahbazi
Department of Pharmaceutical Nanotechnology
School of Pharmacy
Zanjan University of Medical Sciences
Zanjan 45139-56184, Iran
Prof. H. A. Santos
Helsinki Institute of Life Science (HiLIFE)
University of Helsinki
Helsinki FI-00014, Finland
Dr. M.-A. Shahbazi
Zanjan Pharmaceutical Nanotechnology Research Center (ZPNRC)
Zanjan University of Medical Sciences
Zanjan 45139-56184, Iran

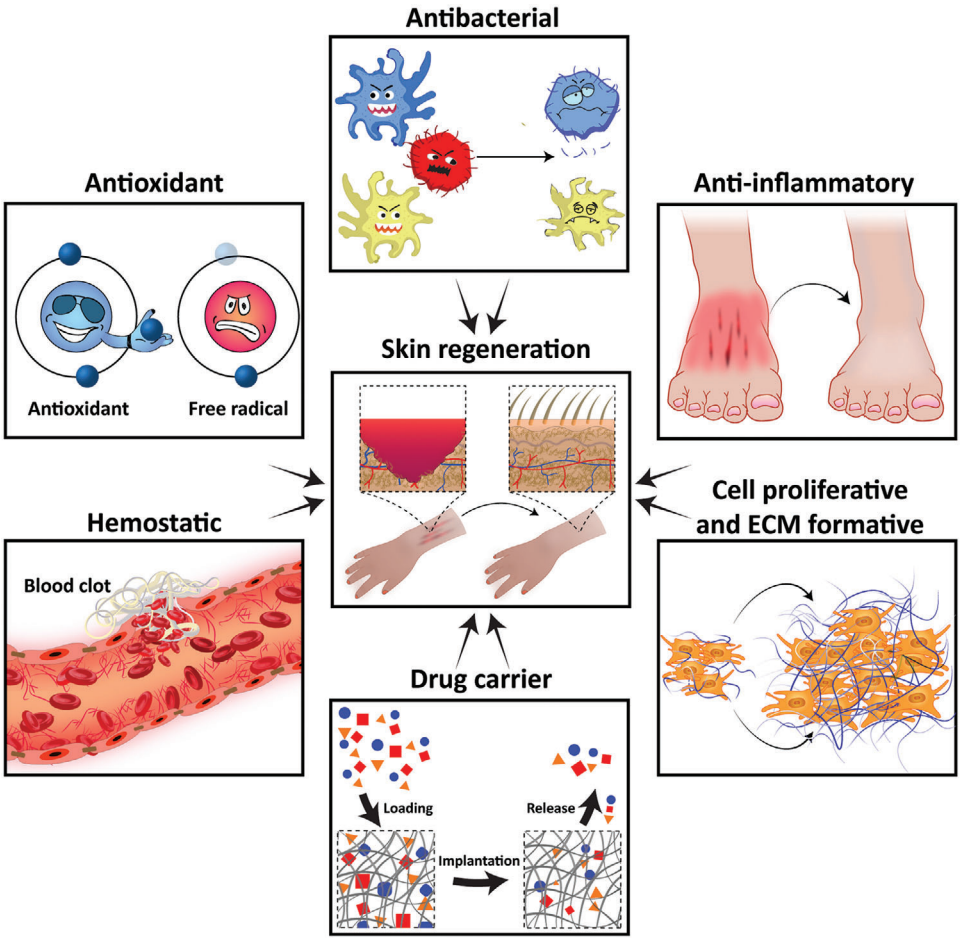

Scheme 1. Multifaceted mechanisms involved in the wound healing effect of the GelTA-Alla hydrogel.

process,[10] rendering low cost and scalability to the composite.[13] Tyrosine and serine amino acids with free hydroxyl groups are present in the structure of PSG that can create abundant physical (noncovalent) hydrogen bonding with TA to increase the strength of the final GelTA hydrogel.[30,37] Proline and 4-hydroxyproline sites are also present in the structure of gelatin for hydrophobic interactions with pentagallyol glucose of TA to further promote the stabilization of the hydrogel after the formation,[38–40] resulting in the fabrication of GelTA by a simple approach without adding any chemical crosslinker. In addition, gelatin has very low cost, low immunogenicity, and high biocompatibility, which are very important criteria for a raw material when the aim is the design of a tissue regenerative product with bench to bedside movement potential.[13] TA is also a generally recognized as safe (GRAS) polyphenol that do not impose toxicity to the host after degradation.[36,38]

For the optimization and characterization purposes, a series of GelTA hydrogels were prepared by adding 1.2 mL of the TA solution at the concentrations of 0.3, 0.4, 0.5, 0.6 g mL^{-1} to 10 mL of gelatin solutions (10% w/v), while stirring to obtain GelTA hydrogel. After preparing the hydrogels, they were characterized with respect to gelation time, yield, gel content, and initial water content. Gelation time was varied between 38.7 ± 6.1 and 10.3 ± 3.0 s, decreasing constantly by the increase of TA concentration (Figure 1c). This has mainly resulted from the faster physical bonding between the TA and gelatin as a function of abundant −OH groups within the reaction solution. The yield (Figure 1d) and gel content (Figure 1e) also demonstrated TA-dependent behavior in which both parameters showed bigger values by the increase of TA concentration. In fact, increasing the TA concentration from 0.3 to 0.6 g mL^{-1} provided more hydroxyl groups for interaction with the polymeric chains of the gelatin and reduced the amount of nonreacted gelatin within the hydrogel structure. Nevertheless, initial water content (Figure 1f) was negligibly altered by the change of TA concentration during the synthesis of the GelTA hydrogel. Since the total weight of the initial materials used for the synthesis of hydrogels was slightly changed by the change of TA concentration and the volume of TA and gelatin solutions were constant in all conditions, very low change on the total weight of the wet hydrogel and initial water content were observed.

2.1.1. Swelling, Water Retention, and Degradation Studies

Hydrogels can be characterized by several physical parameters, such as swelling, water retention, and degradation rate. Swelling property, as one of the most important criteria of hydrogels, affects the release rate of loaded compounds and absorption of

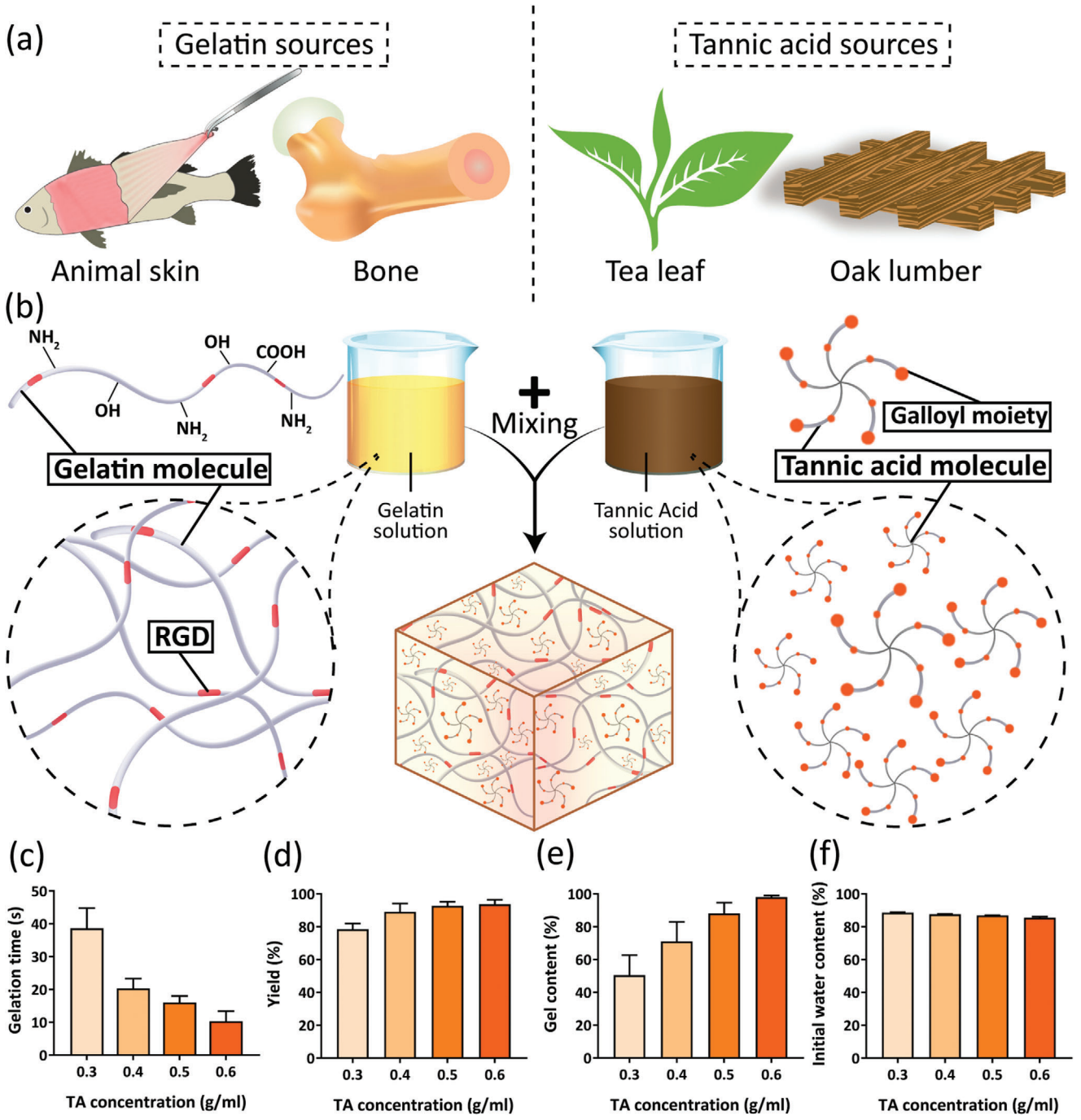

Figure 1. a) Schematic illustration of TA and gelatin sources and b) the synthesis principle of the GelTA hydrogel by hydrogen bonding between the hydroxyl groups of TA and amine and carboxyl groups of gelatin. Hydrophobic interactions between the galloyl moiety of TA and proline and 4-hydroxyproline of gelatin can also assist the formation of GelTA hydrogel. c) Gelation time, d) yield, e) gel content, and f) initial water content, as a function of TA concentration. Gelation time, yield, and gel content were altered by changing the TA concentration, while initial water content remained almost constant in different samples. Data are reported as the mean of three independent experiments ± standard deviation (SD).

wound exudates.[27] The presence of hydrophilic groups in the hydrogel network and higher osmolarity inside the hydrogel compared to the surrounding environment lead to water uptake and swelling of hydrogels.[11] In this study, the swelling assay was performed at two pH values of 5.5 and 7.4 (**Figure 2**a,b). The results showed a very high and fast rate of water uptake by hydrogels at pH 7.4 due to their hydrophilic nature and interconnected porous structure (Figure 2g) that are desirable for the absorption of wound exudates. It is proved that the high swelling capacity enables hydrogels to concentrate clotting factors for the promotion of hemostasis rate after bleeding.[41] The higher TA concentration led to a lower extent of swelling due to the higher

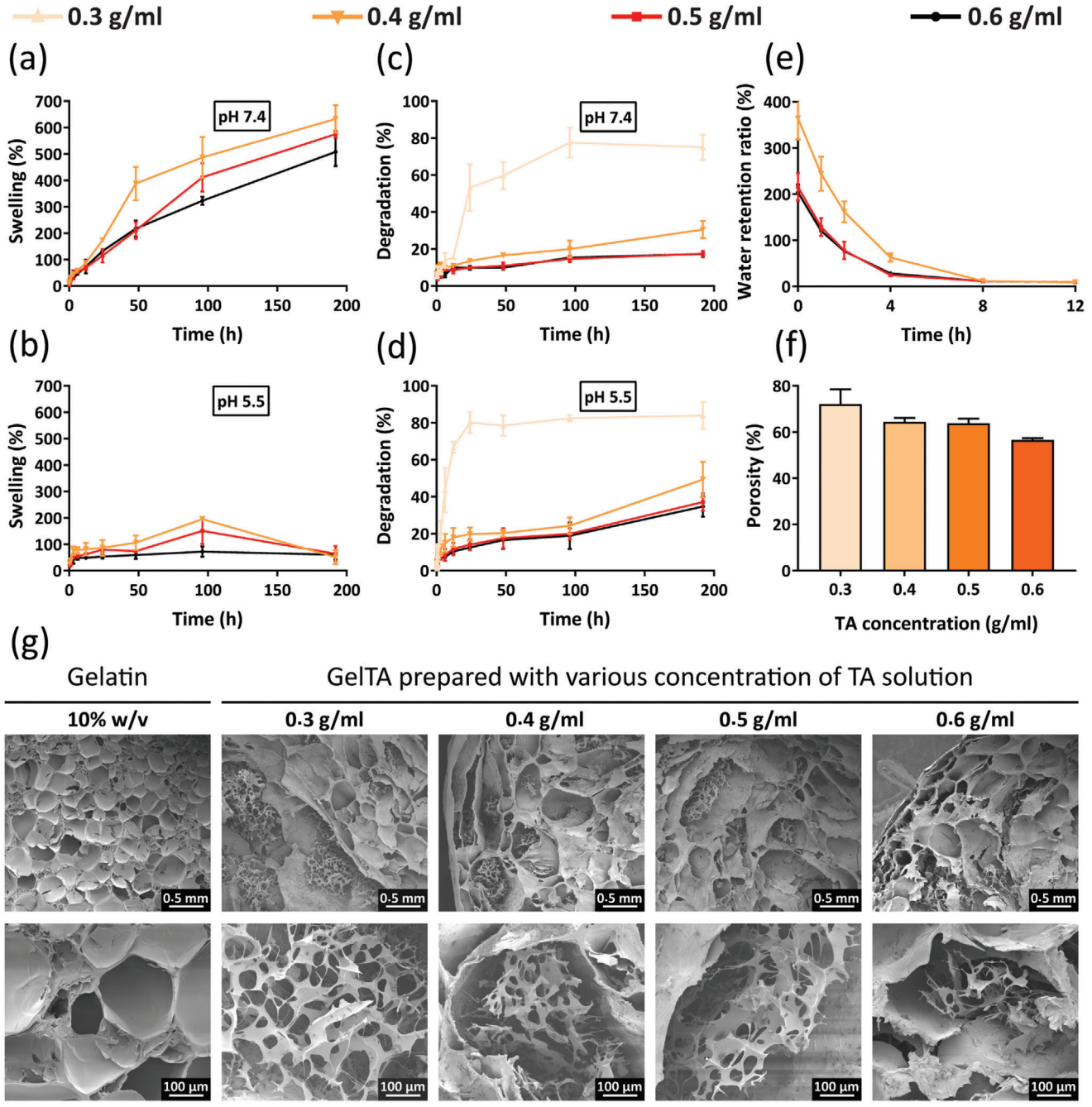

Figure 2. Physicochemical characterization of the GelTA hydrogels. a,b) The swelling percentage of the GelTA hydrogels at the pH values of 7.4 and 5.5. c,d) Degradation trend of the GelTA hydrogels at pH values of 7.4 and 5.5. e) Water retention ratio of the hydrogels over time. f) The porosity percentage of the GelTA hydrogels prepared by different concentrations of the TA solution. All experiments were performed in triplicate and data are reported as mean ± SD ($n = 3$). g) Morphological imaging of the freeze-dried gelatin (10% w/v) and GelTA hydrogels prepared with gelatin (10% w/v) and various concentrations of the TA.

degree of interaction between TA and gelatin chains and reduced porosity (Figure 2f). The extent of swelling was lower at pH 5.5 as compared to pH 7.4. This observation was ascribed to the polyacid nature of TA that could deprotonate at neutral pH, when the number of protonated amine groups of gelatin was reduced and its carboxyl groups were partially ionized to COO^-, resulting in reduced hydrogen bonding, charge repulsion between connected chains of TA and gelatin, and more water penetration into the hydrogel network.[27] In acidic condition, the presence of carboxyl groups and protonated amine groups in the backbone of the gelatin could increase the abundance of hydrogen bonding with TA that, in turn, resulted in the dense connection between TA and gelatin chains and reduced water transfer into the GelTA hydrogel.

Despite of beneficial properties of gelatin for tissue engineering, its low stability, poor mechanical properties, and fast degradation have limited its alone application in regenerative medicine.[21] To circumvent this drawback, physical crosslinking by TA could create stable hydrogels in a concentration-dependent manner (Figure 2c,d). As described earlier and shown in Figure 1e, the gel content, which is representative of the interaction between gelatin and TA, was very low when the TA concentration was 0.3 g mL^{-1}. Therefore, due to the reduced hydrogen bonding and the presence of many free chains of gelatin, a very rapid degradation rate (≈80% within 96 h) was occurred for GelTA hydrogels prepared by TA at the concentration of 0.3 g mL^{-1} (Figure 2c,d). Such a high rate of dissociation did not allow the quantification of swelling rate for this type of GelTA for a long time since the swelling value started to drop down in less than 24 h (data not shown), as a result of high degradation.

The degradability of hydrogels can provide space for cell infiltration, migration, and proliferation, while regulating cell behaviors essential for successful tissue regeneration.[42] The simplest way to change the degradation rate of a hydrogel is the alteration in crosslinker concentration during the synthesis process.[42] In this study, the in vitro degradation was investigated as a function of TA concentration by the measurement of mass loss in specific time intervals post hydrogel incubation in phosphate buffer saline (PBS; pH 7.4 and 5.5). Except for the highly degradable hydrogel prepared by the TA solution of 0.3 g mL^{-1}, other GelTA hydrogels showed that swelling does not induce degradation in the tested time points. In addition, a bit higher degradation despite low swelling behavior of hydrogels at pH 5.5 can be related to the faster hydrolysis of the gelatin chains at acidic pH.[37]

The rate of water evaporation from hydrogel plays a key role in protecting the wound site from moisture loss by retaining the water within the hydrogel network. Beneficially, the rate of re-epithelialization is faster in moist wounds compared to dry wounds since the movement of epithelial cells across moist wounds is more facilitated.[43] Thus, water retention experiment was performed to evaluate the ability of the hydrogel for water holding capacity. The water retention ratio of swollen hydrogel was determined at room temperature. As shown in Figure 2e, with the time increasing, the content of water in all tested GelTA hydrogels was decreased. However, the reduction rates were different and dependent on the concentration of TA within the hydrogel. The rate of water loss was higher in the hydrogel prepared with TA at a concentration of 0.4 g mL^{-1} because of the poor connectivity of the polymeric chains and low crosslinking density as compared to GelTA hydrogels made by TA solutions of 0.5 and 0.6 g mL^{-1}. During the first 4 h, the water retention ratio was decreased by ≈300% for the GelTA prepared with a TA solution of 0.4 g mL^{-1}, while the water loss was less for the other two tested samples during the same time period. In addition, the rate of water loss was faster in the initial time points. This can be explained by the type of water molecules available within the swollen hydrogel. The water molecules in the swollen hydrogels exist in three forms of free water, bound water, and half-bound water. The initial fast rate of water evaporation can be explained by the facile loss of free water molecules from the hydrogel.

2.1.2. Porosity and Morphological Features of the GelTA Hydrogel

High porosity in hydrogels is an important physical property, as it has great impact on cell migration for successful tissue regeneration, nutrition and oxygen supply, and waste removal required for cell survival.[44] Furthermore, hydrogel porosity has a crucial effect on local angiogenesis and affect the mechanical properties of hydrogels.[45] In this study, the percentage of porosity was measured via ethanol displacement method (Figure 2f) since the capillary force allows ethanol to get into the freeze-dried hydrogels.[46] The percentage of porosity for all GelTA hydrogels was greater than 50% with a decreasing trend by the enhancement of TA concentration in the backbone of the hydrogel. While the porosity of the GelTA prepared by 0.6 g mL^{-1} of TA was 56.5 ± 0.8%, this value was 72.1 ± 6.3% for the GelTA hydrogel fabricated by TA at the concentration of 0.3 g mL^{-1}. In fact, increasing the amount of TA, which acts as a cross-linker among gelatin chains, could promote the density and strength of the hydrogel through the porosity reduction.[47]

The pore interconnectivity and pore size of hydrogels also play an important role in tissue engineering.[45] Desirable pore size is important for cell infiltration, proliferation, and migration, while pore interconnectivity is beneficial for vascularization and providing oxygen and nutrients to the cells within the scaffolds' network.[48,49] Scanning electron microscopy (SEM) images displayed highly porous structures with high interconnectivity for all GelTA hydrogels after freeze-drying (Figure 2g). Mesoporous interconnectivity also provides adequate space for drug diffusion from the bulk of the scaffolds.[50] The comparison of SEM images of different GelTA hydrogels indicated no effect of TA concentration on the pore size. Gelatin (10% w/v) without TA was also freeze-dried and imaged by SEM, demonstrating no interconnectivity among the pores. These studies revealed the possibility of designing hydrogels with a broad range of physical properties by the alteration of TA concentration.

After the characterization studies, TA solution with a concentration of 0.5 g mL^{-1} was selected for Alla loading and further experimental investigations. Since Alla was loaded within the hydrogel structure during the gelation process, all drug molecules were entrapped within the polymeric network of the GelTA. Alla can improve the wound healing potential of the GelTA hydrogel due to its triggering effect on cell proliferation and collagen synthesis.[51] The presence of both carboxyl and amine groups in the structure of Alla resulted in its ionic interaction with polymer chains and sustained release of the drug (see Section 2.2). All characterization studies were also performed with the Alla too and it was observed that drug loading has no effect on gelation time, yield, gel content, and initial water content of the GelTA hydrogel. In addition, gel formation and drug loading was tested in different conditions, such as basic environment or low temperature, during the optimization studies to find the optimum formulation for the fabrication of a gel with desirable wound healing effect.

2.1.3. Fourier-Transform Infrared Spectroscopy (FTIR)

Interaction between gelatin, TA, and Alla was evaluated via FTIR spectroscopic analysis (**Figure 3**a). In the spectrum of gelatin,

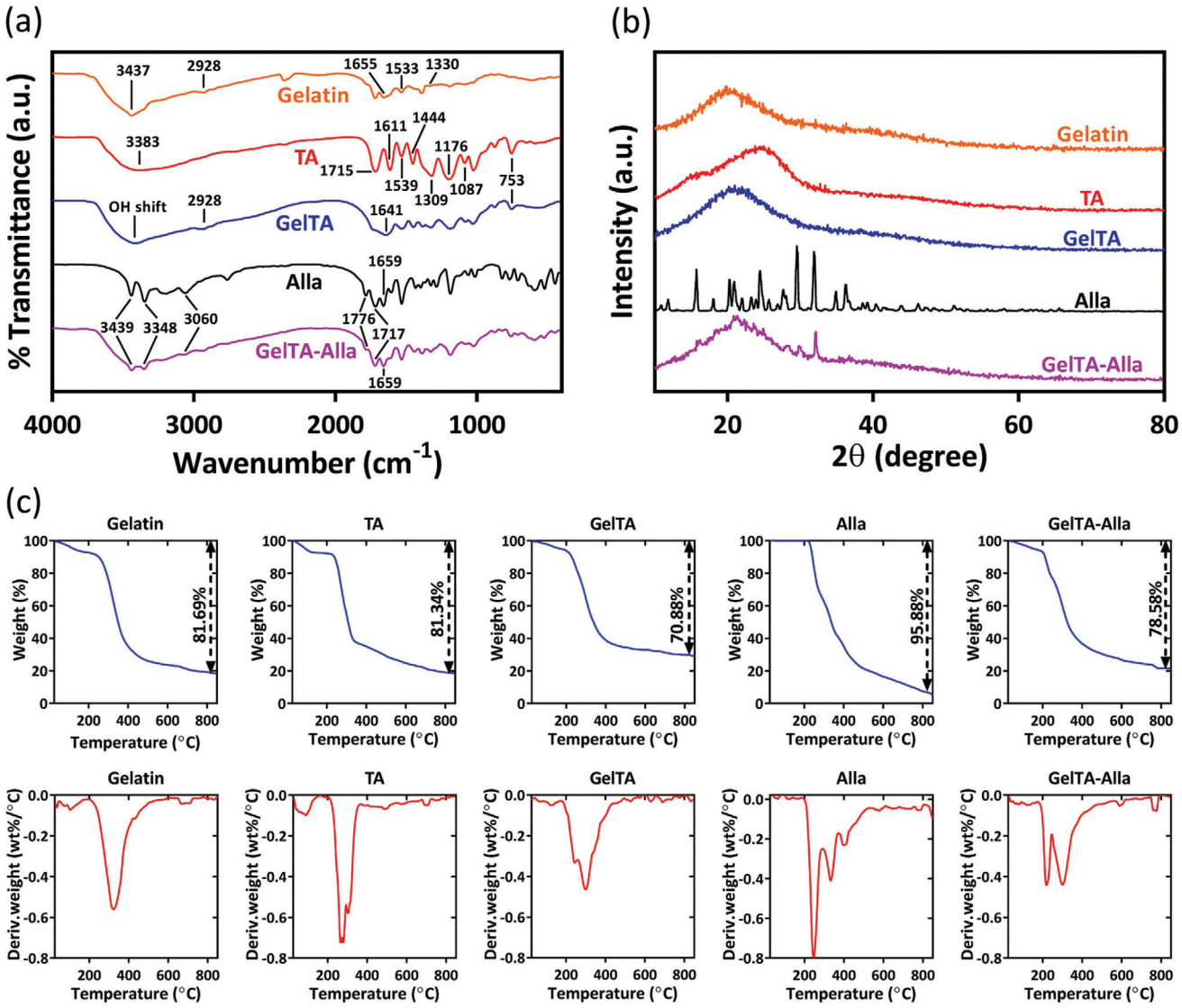

Figure 3. Physicochemical characterization via FTIR, XRD, TGA, and DTG analysis of gelatin, TA, GelTA, Alla, and GelTA-Alla. a,b) FTIR and XRD analysis indicated that gelatin and TA interaction in GelTA could alter the location of bands, confirming gel formation through hydrogen bonding. Due to the drug loading in GelTA-Alla, new bands have emerged when compared to the GelTA. c) TGA (upper blue thermograms) and DTG (lower red thermograms) results confirmed the interaction between TA and gelatin in the GelTA via the increased thermal stability of the hydrogel. The residual weight of all materials at 850 °C are shown in the TGA thermograms. The DTG thermograms are plotted for a better understanding of the rate of material weight changes upon heating up to 850 °C. Overlapped thermograms of gelatin, TA, and GelTA are shown in Figure S1 (Supporting Information) for better understanding of the degradation speed before and after GelTA formation.

a wide band was observed at 3437 cm^{-1} because of the –NH stretching vibration of amide A and free –OH groups in its structure. The bands at 2928, 1655, and 1533 cm^{-1} were due to the C–H stretching vibration of proteins, C=O stretching vibration of amide I, and N–H deformation of amide II, respectively.[52] The band at 1330 cm^{-1} was also attributed to the wagging vibration of proline side chains. In the spectrum of TA, the wide band of –OH stretching vibration was centered at 3383 cm^{-1}. The absorption bands at 1715, 1611, and 1539 cm^{-1} were appeared owing to the stretching vibration of C=O groups of aromatic esters, aromatic C=C stretching, and aromatic C–C stretching, respectively. Bending vibrations for C–H [(in-ring) aromatic] at 1444 cm^{-1}, bending vibrations for O–H at 1309 cm^{-1}, stretching vibrations for C–O (esters, ethers) at 1176 cm^{-1}, C–O of polyols at 1087 cm^{-1}, and C–H out-of-plane deformation of benzene ring at 753 cm^{-1} were also visible in the FTIR spectrum of the TA.[27,53] Since physical hydrogen bonds are the driving forces behind the transformation of gelatin and TA to the GelTA hydrogel, the –OH bands of both TA and gelatin have slightly shifted to lower wavelength after GelTA formation. In addition, the C–H stretching vibration of gelatin at 2928 cm^{-1} and all above-explained bands of TA have appeared in the structure of GelTA. Moreover, the C=O stretching vibration band of gelatin at 1655 cm^{-1} and the absorption bands of TA at 1715 cm^{-1} (stretching vibration of C=O groups in the

aromatic esters of TA) and 1611 cm^{-1} (aromatic C=C stretching) were merged to cause a wide band at 1641 cm^{-1} in the spectrum of GelTA hydrogel. The comparison of FTIR spectra of GelTA-Alla and GelTA demonstrated the emergence of two new bands at 3439 and 3348 cm^{-1} in the former one due to the NH_2 asymmetric and symmetric vibrations of Alla, respectively, confirming successful embedding of the drug within the hydrogel network. The band at 3060 cm^{-1}, which was corresponded to the C–H stretching vibration, could also further confirm the incorporation of the Alla within the GelTA hydrogel. Other peaks at 1776, 1717, and 1659 cm^{-1} in GelTA-Alla hydrogel was attributed to C=O stretching vibrations of Alla.

2.1.4. X-Ray Diffraction (XRD) and Thermal Stability Studies

XRD results (Figure 3b) displayed a broad peak at 19 °θ for gelatin that was due to its triple-helical crystalline structure and indicated its partially crystalline structure. The diffraction peaks at 20–30 °θ in the spectrum of TA indicated its amorphous structure. In the GelTA hydrogel, the diffraction peak of gelatin shifted to 22 °θ, indicating increased amorphous nature of gelatin as a result of crosslinking with TA. By insertion of TA, the breakage of intermolecular interaction between polymer chains was occurred, subsequently resulting in the creation of space between gelatin chains and distribution of the order of crystallinity.[54] Alla showed many diffraction peaks due to its crystalline structure. XRD spectrum of the GelTA-Alla hydrogel demonstrated a remarkable new peak at 32 °θ as compared to the GelTA, confirming the presence of Alla in the hydrogel structure. Other peaks of the Alla were not noticeably observable in the spectrum of the GelTA-Alla hydrogel due to the little amount of Alla that was embedded into the network of the hydrogel. Furthermore, the spectrum of GelTA-Alla hydrogel demonstrated that the GelTA hydrogel could disturb the crystallinity of the Alla.

Thermal gravimetric analysis (TGA) and derivative thermogravimetry (DTG) analysis demonstrated the occurrence of an initial weight loss step for all samples except Alla at temperatures less than 200 °C due to the evaporation of absorbed and crystalline water and any other volatiles (Figure 3c). As a result of the highly hydrophilic nature of gelatin and TA, these two hygroscopic materials can have tendency to absorb moisture from the air. GelTA and GelTA-Alla are also composed of both gelatin and TA, therefore they show same property. In addition, since they have been prepared in aqueous solution, even after drying, few water molecules might remain within the hydrogel network, resulting in initial weight loss at temperatures less than 200 °C. The plot of gelatin displayed a total degradation of 81.7% during the heating process up to 850 °C. The second weight-loss stage for gelatin was observed at 200 to 600 °C due to the thermal decomposition of side and main chains of gelatin. The remained weight in all samples was attributed to char formed under the nitrogen atmosphere. The thermal analysis of TA showed some peaks related to its step by step decomposition at temperatures higher than 200 °C, initiated by decarboxylation reaction at 235 °C.[55] TA degradation showed a maximum of decomposition rate at 270 °C and that was continued until 800°C, leaving about 20% ash. In the GelTA hydrogel, the residual weight was more than 29% at 850 °C, which was higher than the free gelatin and TA. This can be the result of hydrogen bonding between gelatin and TA that restricted chain mobility, which subsequently induces increased thermal stability. This hypothesis was confirmed by DTG, demonstrating lower maximum degradation speed for GelTA (0.46%/°C) than that of pure gelatin (0.56%/°C) and TA (0.72%/°C). More to this, the highest degradation rate of TA (0.72%/°C at 270 °C), which was probably related to the decomposition of the outermost layer of gallic acid units, was significantly reduced as a result of TA inclusion into the gelatin macromolecule chains and the hydrogen bonding between these two materials. The TGA of Alla has shown 3 main stages for its degradation that caused more than 95% of weight loss at 850 °C.[56] The observation of Alla and GelTA degradation peaks in the GelTA-Alla thermogram confirmed Alla loading into GelTA hydrogel. After the loading of the Alla in the GelTA, the residual weight of the hydrogel reduced to the ≈21% at 850 °C (compared to nearly 29% for GelTA before drug loading) that was attributed to the high thermal decomposition of Alla.

2.2. The Release Study and Radical Scavenging Activity of the Hydrogels

The release profiles of TA and Alla from the GelTA hydrogel were studied at two different pH values of 5.5 and 7.4 (**Figure 4**a,b). The results demonstrated that the release of TA from the hydrogel was sustained at the pH value of 7.4 (33.7 ± 1.8% of total TA incorporated into the GelTA hydrogel was released within 336 h) that is desirable for long term inflammatory suppression effect during the wound healing process. The sustained release rate of TA from the GelTA hydrogel can be explained by the interaction between TA and gelatin and the presence of hydrogen bonds in the GelTA hydrogel structure. At pH 5.5, the release rate of TA was very low where only 3.90 ± 0.05% of the total TA was released within 336 h. These results indicated the pH-responsive release of the TA. At the higher pH, deprotonation of polymer and charge repulsion resulted in the hydrogel swelling and TA release from the hydrogel. In contrast, at acidic pH, amine groups of the gelatin are protonated and promote the ionic binding between the hydrogel and free TA within the structure of the GelTA. In nonhealing chronic and infected wounds, the pH of the wound tissue changes to neutral or faintly alkaline (around 7–8.5).[57] This observation suggests that the GelTA hydrogel is useful for the treatment of nonhealing chronic wounds since it can release anti-inflammatory and anti-bacterial TA in the slightly alkaline pH condition. As for Alla, since it possesses amine groups in its structure, its release was not pH-dependent due to its protonation and subsequent repulsion with protonated amine groups of gelatin backbone in the acidic condition. Therefore, the release profile of Alla was similar at both pH values, which is beneficial for its healing effect on both acute and chronic wounds.

Wound site is attacked by enormous free radicals that lead to oxidative stress, inflammation, and cell damage.[58] TA, which was used for hydrogel formation, has antioxidant ability due to its polyphenolic structure.[59] The antioxidant capacity of the Alla is also demonstrated by Selamoglu et al.[60] Therefore, the DPPH scavenging assay was conducted on the TA, Alla, GelTA, and GelTA-Alla to investigate their antioxidant effect while understanding about possible synergistic radical scavenging activity of

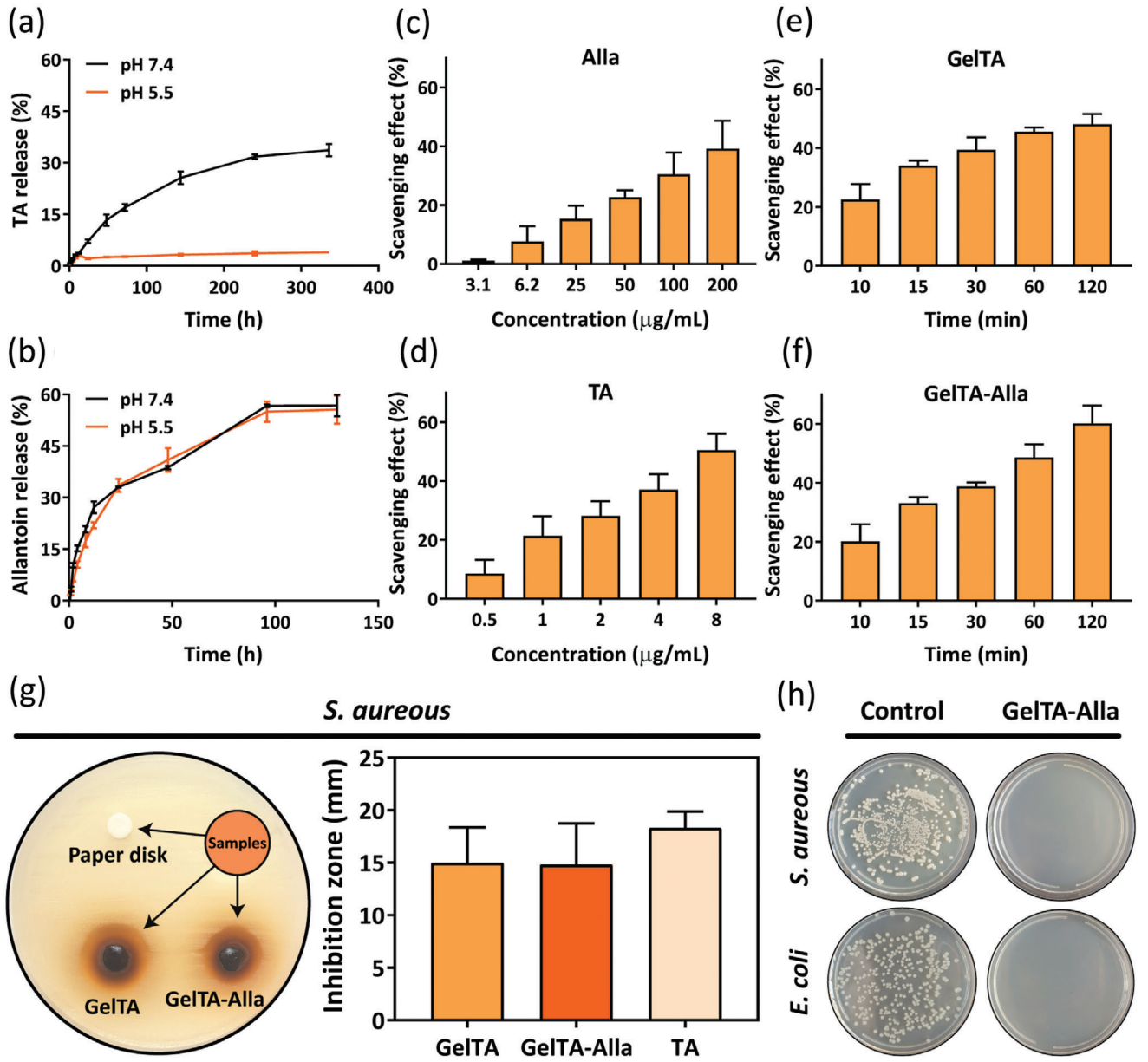

Figure 4. a,b) TA and Alla release from GelTA-Alla hydrogel in PBS medium (pH 7.4 and pH 5.5) at 37 °C. c,d) The percentage of scavenging effect of Alla and TA at different concentrations. e,f) The percentage of scavenging effect of GelTA and GelTA-Alla at 10, 15, 30, 60, and 120 min after incubation in PBS (pH 7.4), measured by the collection of the released medium. g) Photographs and quantitative values of inhibition zone of *S. aureus* around GelTA, GelTA-Alla, and paper disks. Data are reported as the mean of three independent replication of experiments ± SD. h) Photographs of the growth of bacterial colonies of *E. coli* and *S. aureus* on agar plates. In the control groups, both bacteria were treated in PBS (pH 7.4), while in the other group, the bacteria were dispersed in the release medium of GelTA-Alla hydrogels for 24 h.

TA and Alla. As shown in Figure 4c,d, both Alla and TA showed concentration-dependent antioxidant effects. DPPH scavenging effect was 39.2 ± 9.5% for Alla at 200 μg mL^{-1}, while 8 μg mL^{-1} of TA showed 50.5 ± 5.6% of scavenging effect on DPPH, indicating the higher free radical scavenging potency of TA. The high number of OH groups is the main factor that explains the high antioxidant activity of the TA.[59] As shown in Figure 4e,f, antioxidant capacity of GelTA and GelTA-Alla hydrogels were investigated as a function of time by collecting released TA and Alla from the hydrogels into buffer solution. The results were in agreement with the radical scavenging effect of free Alla and TA. After 120 min, DPPH scavenging effect for GelTA-Alla was 60.2 ± 6.1%, whereas it was 48 ± 3.5% for GelTA hydrogel. The higher DPPH scavenging effect of GelTA-Alla could be explained by the combination effect of Alla and TA in the drug loaded hydrogel. Time dependent scavenging effects of both hydrogels were also correlated to the increased concentration of released TA and Alla from the hydrogels over time. These results indicated that GelTA-Alla hydrogel has a great potential for capturing free radicals and possess highly favorable antioxidant properties.

2.3. The Antibacterial Effect of the Hydrogel

The design of actively efficient and safe formulations against virulent bacterial strains that cause wound infections and delay the healing process has remained a challenging task. Thus, the antibacterial ability of wound dressing biomaterials can add more value to their biological effect.[61] Gram-positive *Staphylococcus aureus* (*S. aureus*) and Gram-negative *Escherichia coli* (*E. coli*) are two of the most common colonized biofilms in the chronic wound tissue.[36] Therefore, the antibacterial effect of the GelTA hydrogel was evaluated by two methods on these bacteria to understand their inhibitory effect on the bacterial cells. Measurement of the inhibition zone around the hydrogel in agar diffusion test and the antibacterial effect of the PBS (pH 7.4) medium containing TA released from the hydrogel for 24 h were evaluated. As shown in Figure 4g, the average diameter of the inhibition zone was around 15.0 ± 3.3 mm for GelTA and 14.8 ± 3.9 mm for GelTA-Alla in the *S. aureus* cultured agar plate. In contrast, in the negative control, where just the paper disk was used without TA, the inhibition zone was not observed. To confirm the obtained results are associated with TA release from the hydrogel, the same study was conducted by dropping the TA solution with a similar amount of TA available in the 6 mm hydrogel disk, onto a paper disk. The inhibition zone of TA solution was around 18.3 ± 1.5 mm. This observation not only confirmed the potent antibacterial effect of the TA, but also indicated that the controlled release of TA from the hydrogel, which is attributed to its involvement within the network of the GelTA for the hydrogel formation, would result in slightly reduced antibacterial effect as compared to the free TA. However, the difference was not significant. Nevertheless, it is worthy to point that all TA used during the formation of the hydrogel would not release from it since a large proportion of TA has been involved in the hydrogel backbone and just part of it is freely available for sustained release. This is the main explanation for higher effect of the free TA on the bacteria.

In the second experiment, the release medium of the GelTA-Alla hydrogel was collected after 24 h and then incubated with bacteria for 24 h before visualizing the survival of both Gram-positive and Gram-negative bacteria by culturing them on the agar plate. Bacterial cells incubated in PBS (pH 7.4) for 24 h were considered as negative control groups. As shown in Figure 4h, colonies of *E. coli* and *S. aureus* were not observed on agar plate after 24 h of treatment with TA released from the hydrogel. In contrast, in the negative control group, bacterial colonies were visible and covered the surface of the agar plate. The above results demonstrated that the GelTA-Alla hydrogel possesses excellent antibacterial effect against both *E. coli* and *S. aureus* and this effect is because of TA presence within the structure of the hydrogel. TA is a natural antimicrobial agent[13] that induces bactericidal effect via several mechanisms, including increased destabilization and permeability of the cytoplasmic membrane, as well as destructive interaction with bacterial cell wall proteins and enzyme inhibition.[27] Since antibiotic resistance of bacteria is one the main obstacle for the treatment of infected wounds,[62] the sustained release of TA and its potency can presumably provide better therapeutic condition for infected and chronic wounds as it can enhance the exposure time of bacteria to the TA and provide prolonged antibacterial activity for overcoming the bacterial resistant. Furthermore, the pH-dependent release of TA is advantageous for infected wounds with the pH range of neutral to slightly alkaline (7–8.5) for on-demand drug delivery.[57]

2.4. Cell Viability Studies

Hydrogels prepared by natural polymers, such as collagen, silk fibroin, gelatin, hyaluronic acid, chitosan, alginate, etc., have been intensively studied in the field tissue engineering due to their favorable biocompatibility and biodegradability.[63,64] In this study, gelatin and TA were used as natural materials to fabricate a safe multifunctional hydrogel. The viability studies were performed on 3T3 fibroblast cells at two different time points, 24 and 48 h, through the treatment of the cells by different concentrations of the GelTA and GelTA-Alla hydrogels. Due to the critical role of fibroblast cells in wound healing, these cells were employed in this experiment.[27] For viability assay, the CellTiter-Glo luminescence assay was used, which is a sensitive method for the evaluation of cell viability. As shown in **Figure 5**a,b, both GelTA and GelTA-Alla did not induce any toxicity on the cells and the results indicated that the percentage of viability was higher than 90% in both tested time points for all concentrations. This observation revealed the innate biocompatibility of the GelTA and GelTA-Alla hydrogel since gelatin, as the main component of the hydrogel, is a natural polymer with excellent biocompatibility and low antigenicity.[13,18,65] In addition, TA is a natural biocompatible polyphenol.[13] Although GelTA did not show toxicity on fibroblast cells, the presence of TA in its structure could induce very efficient antibacterial effects as a result of structural and functional differences between eukaryotic and prokaryotic cells.[27] In the GelTA-Alla, the percentage of viability was higher than 100%, which can be explained by the effect of the loaded drug on cell proliferation as a safe and nontoxic compound.[32] The above results demonstrated that not only the GelTA-Alla is safe, but also it can stimulate cell proliferation to accelerate wound healing. In addition, GelTA is favorably biodegradable in vivo, as shown in the Figure S2 (Supporting Information), and can be used not only for wound healing purposes, but also development of implantable drug delivery systems in the future.

2.5. Hemocompatibility Studies

Hemotoxicity is one of the restricting characters for the in vivo application of biomaterials because it can raise the level of free hemoglobin in the blood and subsequently alter the normal function of the kidneys. Thus, hemocompatibility must be tested during the development of novel biomaterials.[66] The in vitro hemolysis assay was performed to evaluate the blood lysing effect of GelTA in different concentrations and time points. As shown in Figure 5c, all tested concentrations up to 800 μg mL^{-1} of GelTA hydrogel demonstrated that the percentage of nonhemolysed red blood cells (RBCs) are above 95%. In addition, after the centrifugation of the GelTA treated RBCs, all samples had a transparent supernatant similar to the RBCs treated with PBS (pH 7.4) as the negative control (example images are shown in Figure 5d). By contrast, RBCs dispersed in deionized water were completely lysed and created a red color in the supernatant. For all samples,

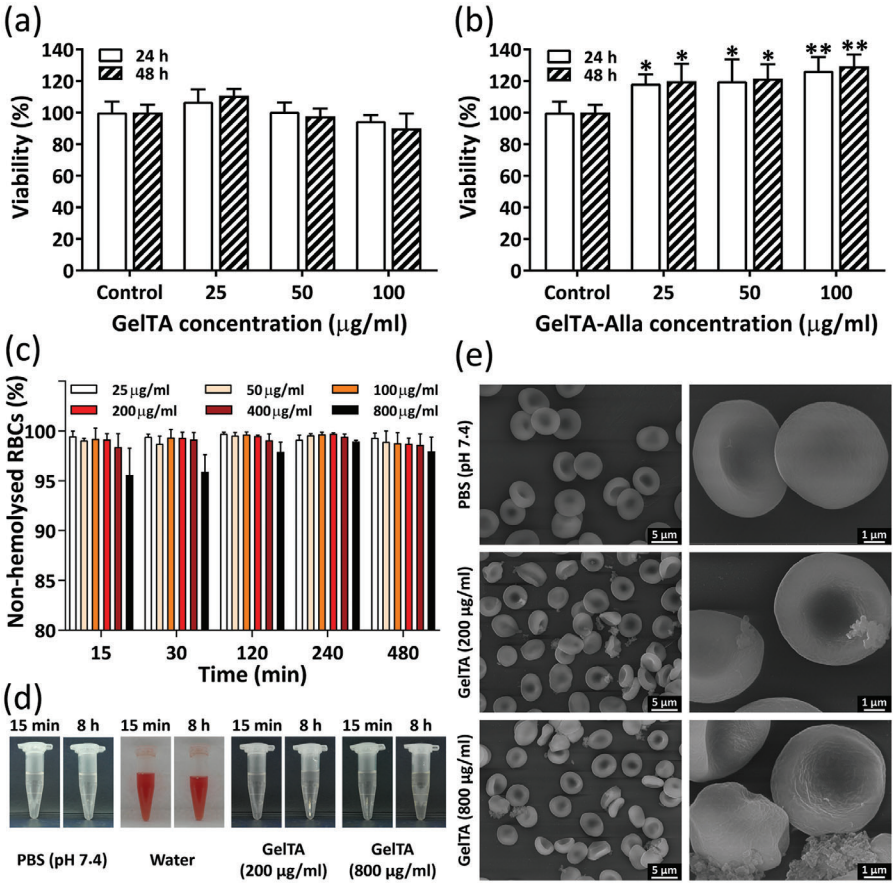

Figure 5. Cell viability of fibroblast cells after exposure to a) GelTA and b) GelTA-Alla hydrogels for 24 and 48 h at 37 °C, quantified by the CellTiter-Glo luminescent assay. Data are reported as mean ± SD ($n = 3$; $*p < 0.05$, $**p < 0.01$ vs negative control group). c) Hemolytic activities were monitored within 480 min of incubation of the human erythrocytes at room temperature with GelTA hydrogel at the concentrations of 25, 50, 100, 200, 400, and 800 μg mL^{-1}. The presence of the lysed hemoglobin in the supernatant was measured by a spectrophotometric method at 540 nm. Data are reported as mean ± SD. d) Photographs of RBC supernatants dispersed in PBS (pH 7.4), water, GelTA with concentrations of 200 and 800 μg mL^{-1}. e) Assessment of morphological change of the RBCs after 8 h of exposure to GelTA at the concentrations of 200 and 800 μg mL^{-1}. The hydrogel attachment on the surface of RBCs was occurred more in 800 μg mL^{-1} as compared to 200 μg mL^{-1}. However, both tested concentrations had a negligible effect on the morphology of the RBCs. On the left, low magnification images are shown and on the right their respective high magnification images. Scale bars are 5 and 1 μm in the left and right columns, respectively.

the percentage of hemolysis was lower than the international permeation level of 5% for biomaterials.[67,68] Therefore, the results indicated that the GelTA formulation has very low hemotoxicity. In addition to blood lysis, the possible impact of GelTA on the morphological change of the RBCs, as a sign of toxicity, was evaluated via SEM imaging (Figure 5e). The results showed that the GelTA did not induce a remarkable change in the morphology of RBCs at both concentrations of 200 and 800 μg mL^{-1} after 8 h of treatment. However, few cells with star-shaped morphology were detected during SEM imaging and concentration-dependent adsorption of GelTA on the RBCs was observed. In general, in vitro toxicity assays highlighted the desirable safety of the GelTA for biomedical applications.

2.6. Blood Clotting Studies

Hemostasis is the first step in the wound healing process in order to prevent blood loss before the initiation of complex mechanisms for cell growth (proliferation), and tissue remodeling (maturation), in which the skin can be repaired.[58] A desirable wound healing process starts with the stimulation of platelet accumulation in the injured tissue and the formation of blood clots for bleeding cessation.[58] In this context, the in vitro blood clotting ability of the GelTA hydrogel was evaluated via the measurement of the blood clotting index (BCI). BCI is a useful index for the evaluation of blood clotting capacity of various materials.[30] In this experiment, the absorbance of free hemoglobin in the supernatant of hydrogels treated with blood was measured to compare the amount of hemoglobin incorporated in the clot formation in the presence of the hydrogel. Therefore, higher absorbance was indicative of lower blood clotting ability.[30] The results showed that GelTA and GelTA-Alla hydrogels have higher blood clotting ability than commercially available gauzes (**Figure 6**a). Besides, Alla loading into the hydrogels did not alter the hemostatic effect of the hydrogel. In vivo hemostatic capacity of the hydrogel was also evaluated by measuring the amount of blood loss and hemostatic time in the rat tail-amputation model. The rats

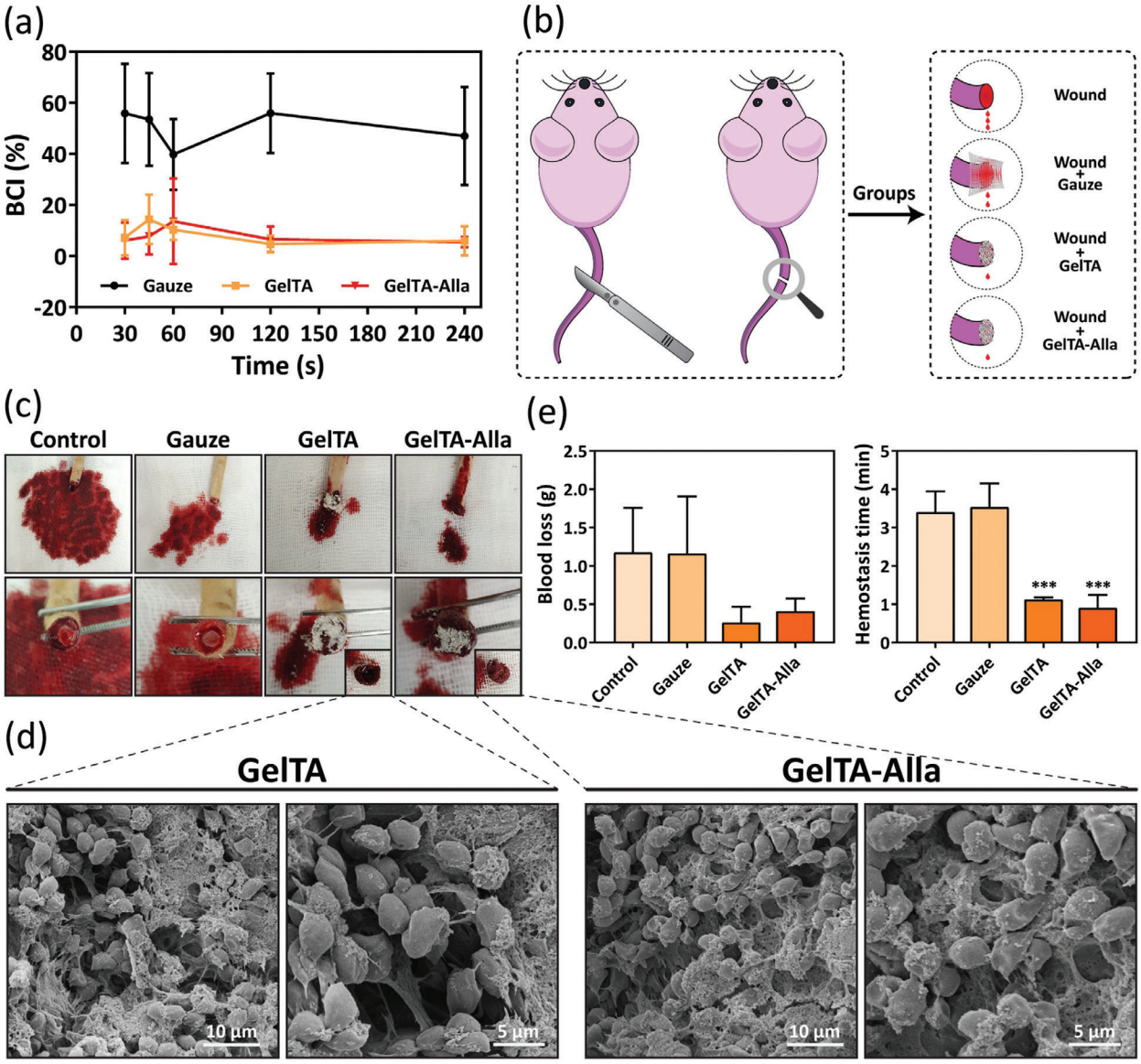

Figure 6. The hemostatic ability of the GelTA and GelTA-Alla hydrogels. a) In vitro hemostatic capacity of gauze, GelTA and GelTA-Alla hydrogels. GelTA and GelTA-Alla groups showed more decline in BCI compared to the gauze group, indicating their better anti-hemorrhage effect. b) Schematic illustration of the in vivo hemostatic study on the tail-amputation rat model for control, gauze, GelTA, and GelTA-Alla groups. c) Photographs of the amount of bleeding in control, gauze, GelTA and GelTA-Alla groups after tail amputation. The insets show the rapid attachment of the blood cells within the GelTA and GelTA-Alla matrices, and subsequent clotting by fibrin formation. d) SEM images of the insets, showing the attachment of the RBCs and other blood cells into the GelTA and GelTA-Alla. The strands of fibrin network surrounding the red blood corpuscles can be observed. e) Quantitative determination of blood loss and hemostasis time. The amount of blood loss and hemostasis time in GelTA and GelTA-Alla groups are very lower than those of the gauze and control group. Statistical analysis was performed by the comparison of the gauze, GelTA and GelTA-Alla with the control group, separately. Data are reported as the mean of three independent experiments ± SD ($n = 3$; $^{*}p < 0.05$, $^{**}p < 0.01$, $^{***}p < 0.001$ vs negative control group).

were divided into four groups and tail amputation was followed by the attachment of a gauze, GelTA, and GelTA-Alla hydrogels on the damaged area, while one group was considered as a negative control without any treatment (Figure 6b). As shown in the photographs of Figure 6c, the amount of blood loss was lower in GelTA and GelTA-Alla groups as compared to gauze and control groups. This observation was confirmed by the measurement of blood loss weight and bleeding time in different groups (Figure 6e). The amount of blood loss was reduced from 1175 ± 582 mg in the control group to 261 ± 207 and 409 ± 166 mg for GelTA and GelTA-Alla hydrogel, respectively. The gauze also did not have any significant inhibitory effect on the bleeding as its value was very similar to negative control animals that did not receive any coverage on their amputated tails (Figure 6e). In addition, the bleeding time was also reduced from higher than 3 min for the control group and gauze treated group to 67.6 ± 3.3 and 54.4 ± 20.4 s for GelTA and GelTA-Alla treated groups (Figure 6e). The above results demonstrated that both GelTA and GelTA-Alla

have higher hemostatic ability than the gauze. When a biomaterial becomes in contact with blood, fibrinogen and other proteins of blood adsorb on the surface of the biomaterial and stimulate platelets' adhesion and aggregation, which further results in the activation of clotting events. The GelTA hydrogel, due to its porous structure and high swelling capacity (Figure 2), can absorb blood and wound exudates quickly and inhibit the escape of RBCs and platelets from the wound site in order to stimulate the formation process of clotting fibrins and induce the trapping of RBCs in the fibrin mesh, as shown in Figure 6d.[69] The blood clotting can be due to the high swelling and fast absorption of water from blood that leads to the creation of a pool of concentrated blood components, consequently aiding the formation of a dense clot. In addition, cationic groups of the gelatin might help the entrapment of negatively charged RBCs into the blood clot as confirmed by SEM images that revealed a dense fibrin mesh formed with RBCs trapped in it via ionic interaction between the GelTA surface and entrapped RBCs. Furthermore, the presence of signaling peptides, such as Arg-Gly-Asp (RGD) in the gelatin structure, allows the recognition of integrin receptors of the cells, resulting in better cell attachment on the hydrogel.[13,70] Consequently, accumulated platelets on the hydrogel would stimulate the blood coagulation cascade.[71] In addition, TA has a vasoconstriction effect[72] and can make interaction with proteins of blood,[30] providing a synergistic effect for the hemostasis ability of GelTA and GelTA-Alla hydrogels. Therefore, cessation of bleeding was a result of vasoconstriction and clot formation.

2.7. In Vivo Toxicity of the Hydrogel

In vivo toxicity was monitored to investigate the translation potential of the hydrogel. For this study, the animals were divided into four groups of control without any wound creation, wound created without any treatment, GelTA-treated wounds, GelTA-Alla-treated wounds. Blood biochemical and hematological parameters were monitored to evaluate the normal function of different organs (**Figure 7**a). Except for the platelet (PLT) level of the GelTA treated group, no significant change was observed in the blood level of RBCs, hemoglobin (HGB), hematocrit (HCT), and platelet (PLT) when compared to the control group. In contrast, an increased number of white blood cells (WBCs), neutrophils (NEUT), lymphocytes (LYMPH), and monocytes (MONO) were observed in all groups as compared to the control, mainly due to the activated protective immunity reactions after the surgery and wound creation.[64] Furthermore, blood level of biochemical indexes and minerals, such as total protein (TP), albumin (ALB), calcium (Ca), phosphor (Ph), blood urea nitrogen (BUN), creatinine (CREA), lactate dehydrogenase (LDH), and alkaline phosphatase (ALP) showed no obvious toxicity of GelTA and GelTA-Alla hydrogels. In addition, the hematoxylin and eosin (H&E) staining of the main organs of rats, including kidney, liver, and spleen indicated no histopathological changes, like necrosis, or alteration of the cellular architecture between tested groups and the control group (Figure 7b). Moreover, due to the intrinsic anti-inflammatory effect of the TA, no inflammation was observed in the wound and its border area after exposure to the hydrogel. Altogether, the GelTA and GelTA-Alla hydrogels did not have any obvious side effect on the functionality of tested organs of rats and induced no metabolic abnormalities.

2.8. In Vivo Wound Healing Study

To evaluate the tissue regenerative ability of the GelTA and GelTA-Alla hydrogels, in vivo studies were performed on rat full-thickness skin wound model (**Figure 8**a). Both the control and Tegaderm groups showed a slow wound recovery process, confirmed by digital photographs of wound area and measuring the relative area of wound remained unrepaired over a 14-day screening period (Figure 8b–d). In contrast, the GelTA and GelTA-Alla treated groups presented an enhanced wound closure rate since ≈98% and 99% of the wound area was healed during the study period. The rate of wound repair was also significantly faster in GelTA and GelTA-Alla groups since 53 ± 2% and 31 ± 5% of the total initial wound zone were remained, respectively, unhealed three days post-surgery. This value was 74 ± 4% and 65 ± 6% for the wound without treatment and Tegaderm groups, respectively. In general, all these results demonstrated a better wound healing effect of the GelTA-Alla than those of other groups by tracing the wound contraction speed over 14 days. This finding was attributed to the combined hemostatic, antioxidant, antibacterial, cell proliferative, anti-inflammatory, and induced ECM formation effect of the GelTA-Alla hydrogel.

The results of H&E staining showed large numbers of inflammatory cells in the control and Tegaderm groups, which also retained a big area of unmatured granulation tissue deposition around the wound (Figure 8e). In comparison, the GelTA and GelTA-Alla groups demonstrated well-proliferated fibroblast, less unmatured granulation tissue around the wound site, and less inflammation and transition of inflammatory cells to the wound bed. These are because the Alla can expedite cell proliferation, and TA can provide a synergistic effect with Alla to scavenge ROS, effectively. In addition, the anti-inflammatory potential of TA via the inhibition of (TNF-α) and (IL-6), and blockage of neutrophil infiltration has been reported in several studies,[27,73,74] which are very beneficial criteria for a wound-healing hydrogel. Following the initial hemostasis, inflammation phase is a critical part of the normal wound healing process, which its prolongation would hamper entering into the proliferative phase and causes delayed wound closure. Therefore, by shortening the inflammation phase we have achieved promoted wound healing. To mechanistically understand how the TA can induce an anti-inflammatory effect, the impact of the GelTA and GelTA-Alla on the macrophages were investigated as explained in the Supporting Information. Our data revealed no meaningful effect of the hydrogels at the concentrations of 50 and 100 μg mL^{-1} on the eliciting of the M2 anti-inflammatory phenotype of macrophages from resting M0 or proinflammatory M1 macrophages (Figure S3, Supporting Information). It was observed that the hydrogels had no effect on the surface expression of CD86 (M1 macrophage marker) and CD206 (M2 macrophage marker). Considering the presence of plenty of immunological pathways in our body, this observation shows that other mechanisms rather than direct M2 polarization effect can be involved in the anti-inflammatory effect of the TA.

Masson's trichrome staining revealed that the density of collagen fibers in the wound bed after 14 days is higher in the GelTA

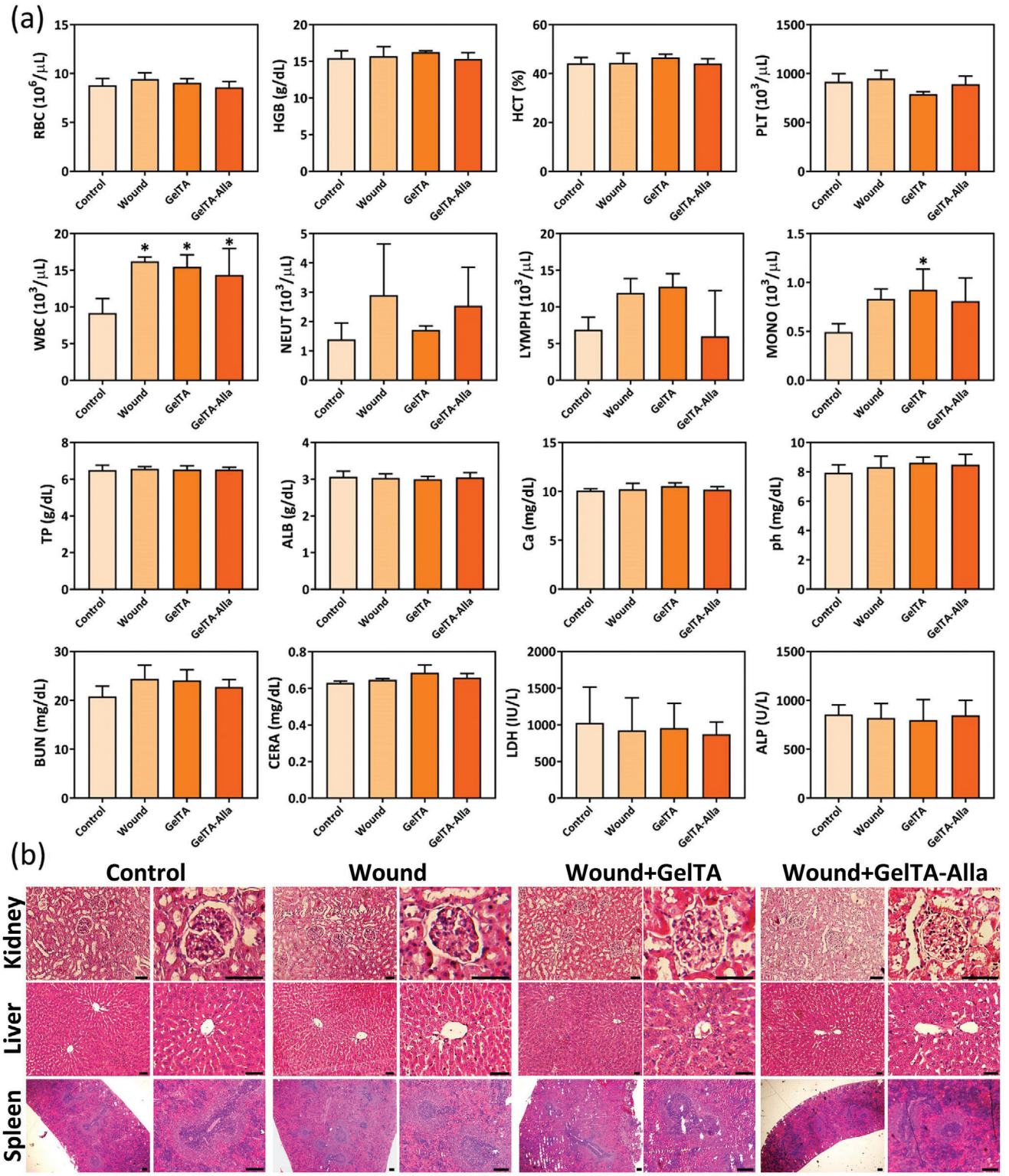

Figure 7. In vivo toxicity evaluation of GelTA, and GelTA-Alla hydrogel in the full-thickness wound rat model. a) Biochemical and hematological factors of animals for control, wound, GelTA, and GelTA-Alla groups. Data are reported as the mean of three independent experiments ± SD ($n = 4$; $^{*}p < 0.05$, $^{**}p < 0.01$, $^{***}p < 0.001$ vs negative control group). b) The H&E staining of kidney, liver, and spleen. Histopathological photographs demonstrated no obvious difference between the control group and the other groups. Scale bar = 50 μm.

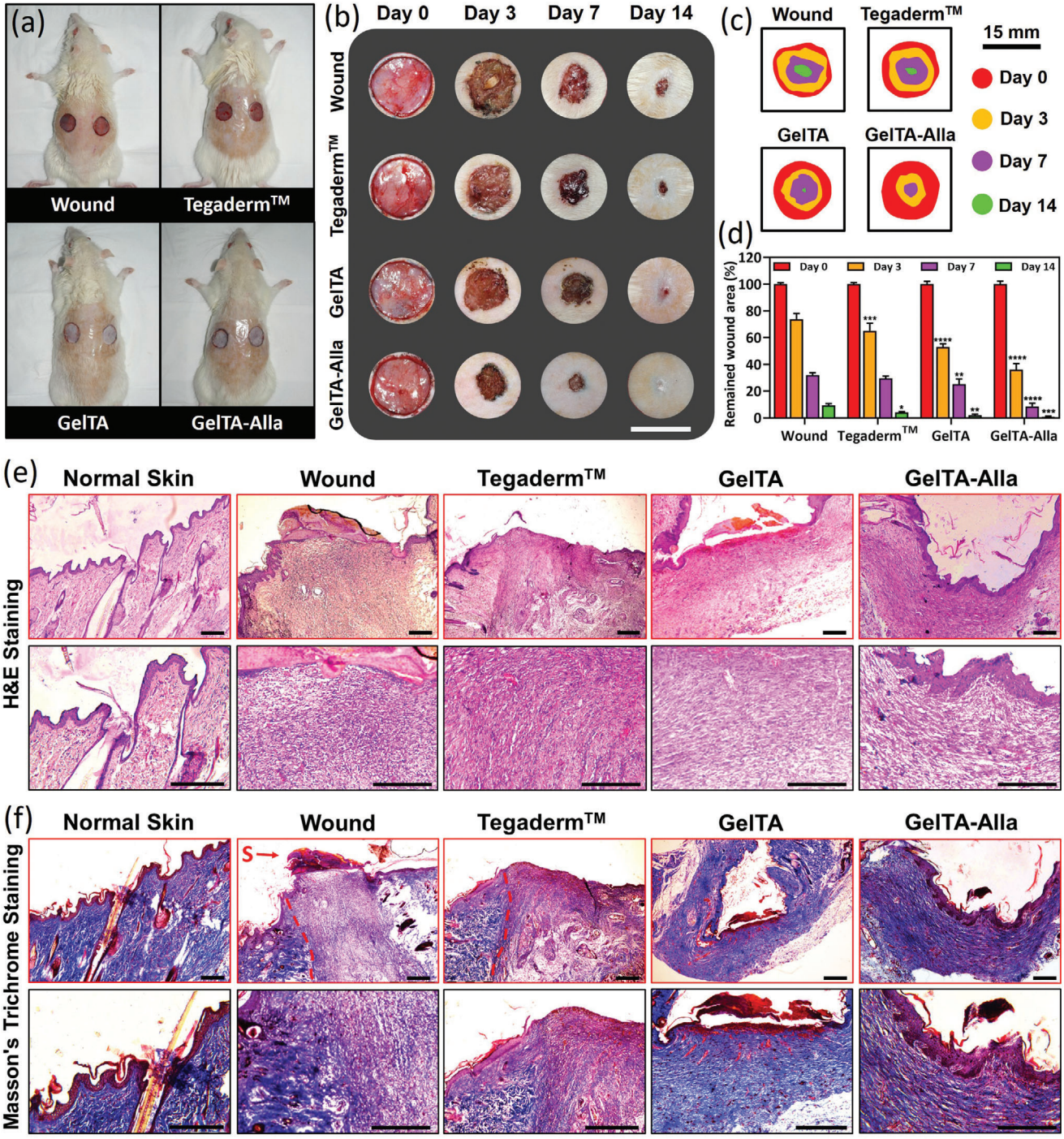

Figure 8. In vivo studies of wound healing process. a) Photographs of animals with full-thickness wounds studied as wound group (without treatment), commercial film dressing (Tegaderm) group, and the groups treated with GelTA or GelTA-Alla for 0, 3, 7, and 14 days. b) Representative photos of different groups over 14 days following surgery. Scale bar = 15 mm. c) Random traces of wound-bed closure of one animal in each group during 14 days for each treatment. d) The relative percentage of remained wound zone over 14 days in different groups ($n = 6$, $^{*}p < 0.05$, $^{**}p < 0.01$, $^{***}p < 0.001$, and $^{****}p < 0.0001$). Statistical analysis was conducted for each day of each group as compared to the corresponding day in the wound group. e) H&E-stained histological sections 14 days post-surgery, showing the granulation tissue, formed epidermal tissue, inflammatory cells, and fibroblast accumulation in the wound bed of different groups. f) Masson's trichrome stained histological sections showing the collagen distribution situation of the normal skin and wound tissue treated differently. S represents the scab. The area on the left side of the red dash lines in the wound and Tegaderm groups represents deposited collagen of the normal skin in the vicinity of the wound area, which is on the right side of the red dash lines. In the sections (e,f), the images with black borders are magnified areas of their corresponded images with the red borders.

and GelTA-Alla treated groups in comparison to other groups, indicating fast wound recovery (Figure 8f). GelTA-Alla group also showed the highest rate of neovascularization, the most thickened epidermis layer, and the highest percentage of collagen formation (Figure S4, Supporting Information). All the above results support the conclusion that the GelTA-Alla is favorable for cell adherence and proliferation, leading to the promoted wound repair process of the defective skin, mainly owing to the cytocompatibility of the hydrogel, the sustained release of the Alla, and induced regeneration of ECM. Indeed, collagen deposition is a critical step for improving ECM formation.[5,75] It is known that collagen is mainly produced by fibroblasts after their migration to the wound bed. Therefore, wound healing scratch assay was performed to understand the role of the GelTA and GelTA-Alla on the stimulation of cell migration to the wound site (Figure S5, Supporting Information) and further confirm the multi-functionality of the developed hydrogels based on all their above-explained effects.

3. Conclusions

In summary, a radical scavenging, hemostatic, antibacterial, and ECM-mimicking bioactive hydrogel was developed. It was shown that similar to polydopamine,[76] TA can improve the mechanical property of gelatin-based hydrogels through noncovalent hydrogen bonding. Moreover, very rapid gel formation, and high capacity of the GelTA for drug loading and delivery was achieved. The hydrogel showed excellent therapeutic effect on wound repair in vivo in a full-thickness skin defect model in terms of wound healing rate, accumulation of inflammatory immune cells, fibroblast migration, epidermis formation, granulation tissue thickness, and collagen disposition. The GelTA hydrogel was successfully synthesized based on one-pot physical hydrogen bonding between gelatin and tannic acid without using any toxic and organic solvent or chemical during the synthesis procedure. The synthesis method was very safe, reproducible, cheap, and scalable. Additionally, tunable physicochemical properties, i.e., swellability, degradability, water retention, gelation time, and porosity, were observed for the GelTA hydrogel by the alteration of TA amount during the hydrogel synthesis. The hydrogel also showed excellent biocompatibility and pH-dependent release of TA from its network at neutral pH, which are desirable criteria for the specific treatment of chronic infected wounds. The loading of Alla within the GelTA hydrogel promoted its biological performance by triggering cell migration and proliferation, inducing keratolytic activity, and promoting collagen formation, while it can also reduce itching and pain at the site of skin injury. This work demonstrates that the GelTA hydrogel is a promising candidate for wound healing applications.

4. Experimental Section

Synthesis of the GelTA Hydrogel: The GelTA hydrogel was prepared through the hydrogen bonding between gelatin and TA. Briefly, gelatin was dissolved in deionized water at 70 °C in a water bath to form a gelatin solution at a concentration of 10% w/v. Then, 1.2 mL of TA solution with different concentrations, prepared in deionized water, was added dropwise into 10 mL of the gelatin solution, while stirring with a spatula to obtain GelTA hydrogel. A series of GelTA hydrogels were prepared using the TA at concentrations of 0.3, 0.4, 0.5, and 0.6 g mL^{-1}. The weight ratios of TA to gelatin were adjusted to 0.36, 0.48, 0.6, and 0.72. Next, the GelTA hydrogels were freeze-dried to obtain dehydrated scaffolds for characterization studies. In addition, gelation time, yield, gel content, initial water content, swelling, water retention, and degradation studies were all performed for the GelTA hydrogel according to the protocols explained in detail in the Supporting Information.

Porosity Measurement and Morphological Characterization: The porosity of the hydrogels was investigated by the solvent displacement method. Briefly, GelTA hydrogels were first prepared and freeze-dried (Eyela, Japan). Next, the freeze-dried samples, with known weight, were immersed in absolute ethanol and kept until complete saturation in ethanol. After the samples were drowned, the percentage of the porosity was calculated following Equation (1)

$$\text{Porosity}\ (\%) = \frac{(W_s - W_d)}{V_s \times \rho\ \text{ethanol}}$$

where, W_s is the weight of the drowned sample after immersing in absolute ethanol, W_d is the weight of the freeze-dried sample, V_s is the volume of the sample after freeze-drying and ρ is the density of ethanol.

The morphology of the freeze-dried hydrogels and their pores were also visualized by SEM (Quanta 250 FEG, USA) by excising thin sections of the samples and coating with a thin layer of gold.

FTIR, XRD, TGA, and DSC Analysis: The interaction between gelatin, TA, and Alla was investigated by FTIR (Bruker, Germany) to confirm hydrogel formation and drug loading. The ATR–FTIR spectra were recorded in the wavenumber region of 4000–400 cm^{-1} at room temperature. In order to study the crystallinity of the drug-loaded GelTA hydrogel, XRD analysis of gelatin, TA, Alla, GelTA, and GelTA-Alla was performed using XRD (PW 1730, Philips, Holland) at room temperature with 2θ range of 10–80 °θ. To investigate the thermal degradation of initial materials and their conjugates, TGA (SDT-Q600, USA) study was conducted with the heating temperature range of 30 to 850 °C and a heating rate of 10 °C min^{-1} under nitrogen atmosphere. Phase transitions were also investigated by DTA in the temperature range of 30 to 850 °C and the heating rate of 10 °C min^{-1} under nitrogen atmosphere.

Drug Loading and Release Studies: The loading of Alla into the hydrogel was conducted by adding 84 mg of the drug into 5 mL of the deionized water and stirring at 50 °C till a transparent solution was obtained. Then, gelatin (500 mg) was added to the solution and stirred for complete dissolution. Next, TA solution (0.5 g mL^{-1}, 0.6 mL) was added to gelatin-drug solution dropwise while mixing the sample with a spatula to form homogenous Alla-loaded GelTA hydrogel. All experiments were performed using this drug loaded hydrogel.

The release of TA from the GelTA hydrogel was investigated in different PBS solutions with pH values of 5.5 and 7.4 using UV–Vis spectroscopy (Genesys 10-S, USA). Dried GelTA hydrogel (0.1 g) was immersed in 40 mL of PBS and incubated under shaking (100 rpm) at 37 °C. At pre-determined time points (0.5, 1, 2, 4, 8, 12, 24, 48, 72, 144, 240, and 336 h), 1 mL of release medium solution was withdrawn for the determination of the TA released from the hydrogel. In all time points, the withdrawn volume was replaced with fresh PBS buffer to maintain the total volume of the release media constant. After sampling, the aliquots were centrifuged for 3 min at 7000 rpm and the cumulative percentage of released TA in the supernatants was quantified using UV–Vis spectroscopy at 274 nm by dividing the amount of TA releases at each time point to the total amount that was present in the initially dried hydrogel. A calibration curve was prepared for the quantification of TA release.

As for the Alla release study, high-performance liquid chromatography (HPLC; Waters 1525, USA) was used after following the above-explained protocol for TA release. A reverse-phase column (C_{18}; 250 × 4.6 mm, 5 µm) and a mobile phase of phosphate buffer with the pH value of 3, by isocratic elution and under a flow rate of 0.5 mL min^{-1} was used to detect the Alla using a UV detector at 210 nm.

Antioxidant Activity of the GelTA and GelTA-Alla: The antioxidant capacity of TA, Alla, GelTA and GelTA-Alla hydrogel was investigated via

DPPH radical scavenging assay to confirm their ability for capturing free radicals. Briefly, a DPPH solution with a final concentration of 0.25×10^{-3} M in ethanol was prepared. Next, dried GelTA and GelTA-Alla hydrogels (0.1 g) were immersed in PBS (40 mL; pH 7.4) and incubated under shaking at 100 rpm (37 °C). At predetermined time points, sampling from the release media of GelTA and GelTA-Alla was conducted similar to the release study. DPPH solution (333 µL) was then mixed with 1000 µL of the release media and incubated in dark at room temperature for 40 min after vortexing. The absorbance of the mixture against blank was recorded at 517 nm using UV–Vis spectroscopy (Genesys 10-S, USA) and the percentage of DPPH scavenging effect was calculated following Equation (2)

$$\text{DPPH Scavenging effect } (\%) = \left(1 - \frac{A_s}{A_c}\right) \times 100$$

where, A_s is the sample absorbance and A_c is the control absorbance. The mixture of DPPH solution (333 µL) and PBS (1000 µL; pH 7.4) that was incubated in dark at room temperature was considered as a control sample. A similar study was performed for the solutions of TA and Alla with known concentrations to enable the interpretation of the obtained results from the hydrogel and understanding the origin of the antioxidant effect of the hydrogel.

Antibacterial Studies on GelTA Hydrogel: *S. aureus* (ATCC 25923) and *E. coli* (ATCC 25922) were used as Gram-positive and Gram-negative bacteria, respectively, to evaluate the antibacterial capacity of the hydrogel. Both bacteria were cultured at 37 °C in sterilized nutrient broth under shaking at 150 rpm overnight. Then, using normal saline (0.9% w/v), bacterial suspension was diluted to achieve the concentration of 1.5×10^8 CFU mL^{-1}. Sterile swabs were used to uniformly disperse 100 µL of the bacterial suspension onto an agar plate. Afterward, cylindrical GelTA hydrogel disks (6 mm diameter) with the same size, thickness and shape were prepared and sterilized under UV-light before placing them on top of microorganism-inoculated agar plates. Paper disks with the same size were used as a negative control. Besides, to identify the role of TA in the antibacterial activity of the hydrogel, 9.75 µL of TA solution (0.5 g mL^{-1}), which contains a similar amount of TA available in the 6 mm hydrogel disks, was dropped onto a paper disk and placed on the agar plate. Samples were then incubated for 24 h at 37 °C before measuring the diameter of the inhibition zone around the paper disks to assess the inhibitory effect of the hydrogel on the bacteria.

In another antibacterial assay, the effect of the hydrogel on the survival of *E. coli* and *S. aureus* bacteria was evaluated. Dried hydrogels were initially sterilized by UV light ($\lambda = 420$ nm) for 5 min. Next, 100 mg of the dried hydrogels were put into 20 mL of sterilized PBS (pH 7.4) solution and incubated at 37 °C under stirring at 100 rpm. After 24 h, the release medium was withdrawn and mixed with 1 mL of bacterial suspension with a concentration of 10^6 CFU mL^{-1} and incubated further for 24 h at 37 °C. PBS buffer (20 mL; pH 7.4) mixed with 1 mL of bacterial suspension was used as a negative control. After the incubation time, samples were diluted 50 times and 100 µL of the diluted media was spread on an agar plate and further incubated for 24 h at 37 °C before visualizing the colony-forming units on the agar plates.

Cell Viability Test: For this study, fibroblast cells were used due to their vital effect during the wound healing process. Cells were cultured in Dulbecco's Modified Eagle's Medium (DMEM) that was enriched with 10% v/v fetal bovine serum (FBS), 100 IU mL^{-1} penicillin, 1% of L-glutamine, 1% of nonessential amino acids, and 0.1 mg mL^{-1} streptomycin. To start the study, 2×10^5 cells mL^{-1} of the fibroblast suspension were prepared in DMEM culturing medium. Afterward, 100 µL of this suspension was poured into 96 well plates and left in the incubator to attach overnight. After removing the cell media, 100 µL of hydrogel suspensions prepared from the powdered freeze-dried GelTA and GelTa-Alla with concentrations of 25, 50, and 100 µg mL^{-1} were added into the wells and incubated for 24 and 48 h at 37 °C in the incubator. The well plates were then taken out from the incubator and 100 µL of the CellTiter-Glo luminescence reagent (Promega, USA) were poured into each well. Afterward, plates were shaken for 2 min and left in the static condition for 15 min, while protected from the light. Finally, the luminescence was recorded using a Varioskan Flash (Thermo Fisher Scientific Inc., USA). Hank's balanced salt solution-(4-(2-hydroxyethyl)-1-piperazineethanesulfonic acid) (HBSS-HEPES) buffer solution as negative control and 1% of Triton X-100 as positive control were used for the viability study and all conditions were conducted three times.

Hemocompatibility of the GelTA Hydrogel: Hemocompatibility of the hydrogel was investigated via measuring the absorbance of released hemoglobin after the RBC lysis. In this assay, anti-coagulated fresh human whole blood was collected from a healthy volunteer and used within 2 h post blood collection. To obtain RBCs, 20 mL of PBS buffer (pH 7.4) was added to 10 mL of whole blood and the mixture was centrifuged at 3000 rpm for 6 min after gentle mixing. RBCs were then collected from the bottom of the centrifuged falcon tubes and the same protocol was repeated 5 times with 1:2 ration of the RBC to the PBS buffer (pH 7.4). Next, RBCs with a concentration of 5% v/v were prepared by diluting them in the fresh PBS buffer (pH 7.4). Dried GelTA and GelTA-Alla hydrogels that were particulated by a grinder were then dispersed in the PBS buffer (pH 7.4) at different concentrations. The suspension was then very gently mixed with the RBC suspension at a 1:1 v/v ration to reach the final concentrations of 25, 50, 100, 200, 400, and 800 µg mL^{-1} of the GelTA and GelTA-Alla in a 1.5 mL tube.

After incubating at room temperature for 15 min, 30 min, 2 h, 4 h, and 8 h, the samples were centrifuged at 3000 rpm for 7 min. The supernatants (150 µL) were transferred to a 96 well plate and the absorbance of the samples was recorded at 540 nm using a microplate reader (Infinite M200, Austria). The percentage of hemolysis was calculated for each sample using Equation (3):

$$\text{Hemolysis } (\%) = \frac{(A_s - A_b)}{(A_p - A_b)} \times 100$$

where, A_s is the sample absorbance, A_b is the absorbance of negative control, and A_p is the absorbance of the positive control. In this assay, fresh PBS buffer (pH 7.4) and deionized water were used as the negative and positive control, respectively.

To evaluate the morphological alteration of RBCs after treatment with GelTA hydrogels, 0.5 mL of the hydrogel dispersions with the concentration of 400 and 1600 µg mL^{-1} were mixed with 0.5 mL of RBC suspension (5% v/v) to achieve the final concentrations of 200 and 800 µg mL^{-1}. After incubation at room temperature for 8 h, the samples were centrifuged at 3000 rpm for 7 min, followed by fixation using 4% formaldehyde for 2 h at room temperature. The samples were then dehydrated by immersing treated RBCs with increasing concentrations of 50%, 60%, 70%, 80%, 90%, and 99.7% ethanol for 5, 10, 15, 20, 25, and 30 min, respectively. Afterward, cell suspensions were spread on coverslips, dried at room temperature, and coated with gold. Finally, the samples were visualized under the SEM instrument (Quanta 250 FEG, USA).

In Vitro and In Vivo Blood Clotting Effect of the GelTA: In vitro blood clotting ability of the hydrogel was investigated using the BCI experiment method. The pre-weighed powder of freeze-dried GelTA and GelTA-Alla hydrogel (50 mg) and pre-weighed gauze (50 mg) were placed into falcon tubes and pre-warmed at 37 °C for 5 min. Next, anti-coagulated blood (100 µL) was added dropwise on the surface of samples gently, followed by adding 12.5 µL $CaCl_2$ (0.2 mol L^{-1}). After incubation at 37 °C for 30, 60, 120, and 240 s, 10 mL of deionized water were added very gently inside the falcon tubes and then centrifuged at 1000 rpm for 5 min. Afterward, the absorbance of the supernatant was obtained at 540 nm using UV–Vis spectroscopy (Genesys 10-S, USA). The blood without the hydrogel or gauze was considered as a reference for calculating BCI using the Equation (4)

$$\text{BCI } (\%) = \frac{A_s}{A_r} \times 100$$

where A_s is the absorbance of supernatant in hydrogel or gauze treated samples, and A_r is the absorbance of supernatant in the reference sample. In this experiment, lower BCI indicates better blood-clotting capacity. All samples were evaluated in triplicate.

The in vivo hemostatic potentials of GelTA and GelTA-Alla hydrogels were evaluated using the rat tail-amputation model.[16] For this assay, 16 male Sprague-Dawley rats with the weight of 230–250 g were amputated from tail and randomly divided into groups treated with gauze, GelTA, GelTA-Alla, and a group without any treatment as negative control. Before the experiment, the animals were anesthetized by intraperitoneal (IP) injection of 0.25 mL of ketamine (50 mg mL^{-1})-xylazine (20 mg mL^{-1}) cocktail (6:4 v/v). Then, a surgical cutting tool was used to cut 50% length of tail, followed by leaving the tail in air for 15 s to make sure of normal blood loss. Next, gauze, GelTA, GelTA-Alla and for one group no treatment were applied to investigate the hemostasis time and blood loss for all groups.

In Vivo Toxicity: In all in vivo studies, animals were housed in an animal room for one week, before starting the experiments, to allow their adaptation to the new environment. During the studies, 12 h light/dark daily cycle, an environmental temperature of 21–23 °C, and relative humidity of 50–60% were applied in the animal room. Principles of laboratory animal care were followed and all the procedures were in accordance with ethical standards and protocols accepted by the Committee of Animal Experimentation guidelines of Zanjan University of Medical Sciences, Zanjan, Iran (ethical code: IR.ZUMS.REC.1398.234).

In vivo toxicity of the hydrogels was evaluated in full-thickness wound model of rat. For this purpose, 16 male Sprague-Dawley rats with a weight range of 230–250 g were divided into four groups, including control without wound creation, wound without any treatment, wound treated with GelTA, and wound treated with GelTA-Alla. The animals were first anesthetized by IP injection of 0.25 mL of ketamine (50 mg mL^{-1})-xylazine (20 mg mL^{-1}) cocktail (6:4 v/v). Then, a full-thickness wound with a 2 cm diameter was created onto the dorsal region of all animals except the control group. For the animals in the wound without hydrogel treatment, no animal received the hydrogels, while the GelTA and GelTA-Alla hydrogel were applied to the wounds in other groups. After 14 days, 2 mL of blood was collected from animals in all groups for blood biochemistry and hematological monitoring. Afterward, the animals were sacrificed and main organs, such as liver, kidney, and spleen were collected for histological assessment of morphological changes in the tissues. Organs were first fixed in a 4% formaldehyde solution overnight, dehydrated, embedded in melted paraffin, mounted on a microtome, and cut into thin slices for H&E staining and visualization under optical microscopy (Olympus Bx51, Japan).

In Vivo Wound Healing Assessment: Full-thickness wounds were used for the evaluation of the GelTA and GelTA-Alla hydrogels on wound healing. In this experiment, 24 male Sprague-Dawley rats were randomly divided into 4 groups (6 animals per group), including wound without any treatment, Tegaderm treated group, GelTA treated group, and GelTA-Alla treated group. The animals were anesthetized by IP injection of 0.25 mL of ketamine (50 mg mL^{-1})-xylazine (20 mg mL^{-1}) cocktail (6:4 v/v). After shaving the hair of animals, two full-thickness round wounds, with a diameter of 1.5 cm were created in the dorsal region of rats on either side of the midline. After surgery and covering the wounds of different groups with Tegaderm, GelTA, and GelTA-Alla, the animals were fed separately to prevent touching the wound tissue. The wounds were monitored on days 0, 3, 7, and 14 after surgery and digital photographs were taken for the measurement of the wound surface area in different groups using ImageJ software. On day 14, the rats were sacrificed by excessive anaesthesia and the wound area with regenerated tissue and the material-host tissue interface were harvested and fixed in paraformaldehyde (4%) overnight. The samples were then embedded in paraffin after dehydration and the blocked samples were sectioned by a microtome (YD-1508A, Leica, Germany), before following the standard protocols of H&E and Masson's trichrome staining for histological evaluation and collagen deposition visualization, respectively.

Statistical Analysis: At least three independent replication for each data set of all experiments were performed and results are reported as mean ± SD. Statistical analysis was performed using GraphPad Prism via the Dunnett's post-hoc test as part of one- or two-way ANOVA at the probabilities of $*p < 0.05$, $**p < 0.01$, $***p < 0.001$, and $****p < 0.0001$ to show the levels of statistically significance.

Supporting Information

Supporting Information is available from the Wiley Online Library or from the author.

Acknowledgements

Z.A. acknowledges financial support from the School of Pharmacy, Zanjan University of Medical Sciences, Zanjan, Iran, under the framework of the thesis project (No. A-12-1296-2) with the ethical code of IR.ZUMS.REC.1398.234. P.F. acknowledges the Finnish Cultural Foundation for a research grant (decision no. 00190246), and the financial support from the Orion Research Foundation. H.A.S. acknowledges the financial support from the HiLIFE Research Funds, the Sigrid Jusélius Foundation, and the Academy of Finland (Grant No. 317042). M.-A.S. acknowledges the financial support from the Academy of Finland (Grant No. 317316). The authors thank the Electron Microscopy Unit and the Flow Cytometry Unit of the Institute of Biotechnology, University of Helsinki, for providing the necessary laboratory facilities and assistance.

Conflict of Interest

The authors declare no conflict of interest.

Keywords

allantoin, anti-bacterial hyrdogels, anti-hemorrhage, hydrogels and gelatin, tannic acid, wound dressing

Received: July 1, 2020
Revised: August 4, 2020
Published online:

[1] J. Kang, J. Hu, R. Karra, A. L. Dickson, V. A. Tornini, G. Nachtrab, M. Gemberling, J. A. Goldman, B. L. Black, K. D. Poss, *Nature* **2016**, *532*, 201.
[2] E. J. Lee, B. Kang, S. Na, J. Yeon, C. Gwon, A. G. Mikos, Y. Bin, *Prog. Mater. Sci.* **2017**, *89*, 392.
[3] X. Zhao, H. Wu, B. Guo, R. Dong, Y. Qiu, P. X. Ma, *Biomaterials* **2017**, *122*, 34.
[4] N. X. Landén, D. Li, M. Ståhle, *Cell. Mol. Life Sci.* **2016**, *73*, 3861.
[5] G. Chen, Y. Yu, X. Wu, G. Wang, J. Ren, Y. Zhao, *Adv. Funct. Mater.* **2018**, *28*, 1870233.
[6] M. A. Shahbazi, M. P. A. Ferreira, H. A. Santos, *Nanomedicine* **2019**, *14*, 2269.
[7] Z. Liu, Y. Li, W. Li, W. Lian, M. Kemell, S. Hietala, P. Figueiredo, L. Li, E. Mäkilä, M. Ma, J. Salonen, J. T. Hirvonen, D. Liu, H. Zhang, X. Deng, H. A. Santos, *Mater. Horiz.* **2019**, *6*, 385.
[8] J. He, Y. Qiao, H. Zhang, J. Zhao, W. Li, T. Xie, D. Zhong, Q. Wei, S. Hua, Y. Yu, K. Yao, H. A. Santos, M. Zhou, *Biomaterials* **2020**, *234*, 119763.
[9] H. Kim, S. Y. Wang, G. Kwak, Y. Yang, I. C. Kwon, S. H. Kim, *Adv. Sci.* **2019**, *6*, 1900513.
[10] E. A. Kamoun, E. R. S. Kenawy, X. Chen, *J. Adv. Res.* **2017**, *8*, 217.
[11] I. P. Harrison, F. Spada, *Pharmaceutics* **2018**, *10*, 71.
[12] P. Thangavel, B. Ramachandran, S. Chakraborty, R. Kannan, S. Lonchin, V. Muthuvijayan, *Sci. Rep.* **2017**, *7*, 10701.
[13] Y. Zheng, Y. Liang, D. Zhang, X. Sun, L. Liang, J. Li, Y. N. Liu, *ACS Omega* **2018**, *3*, 4766.
[14] E. Brauer, E. Lippens, O. Klein, G. Nebrich, S. Schreivogel, G. Korus, G. N. Duda, A. Petersen, *Adv. Sci.* **2019**, *6*, 1801780.

[15] D. S. Yoon, Y. Lee, H. A. Ryu, Y. Jang, K. M. Lee, Y. Choi, W. J. Choi, M. Lee, K. M. Park, K. D. Park, J. W. Lee, *Acta Biomater.* **2016**, *38*, 59.
[16] X. Zhao, B. Guo, H. Wu, Y. Liang, P. X. Ma, *Nat. Commun.* **2018**, *9*, 2784.
[17] H. J. Jang, Y. M. Kim, B. Y. Yoo, Y. K. Seo, *J. Biomater. Appl.* **2018**, *32*, 716.
[18] Y. Dong, A. Sigen, M. Rodrigues, X. Li, S. H. Kwon, N. Kosaric, S. Khong, Y. Gao, W. Wang, G. C. Gurtner, *Adv. Funct. Mater.* **2017**, *27*, 1606619.
[19] K. Yue, G. T. Santiago, A. Tamayol, N. Annabi, A. Khademhosseini, W. Hospital, S. Arabia, *Biomaterials* **2015**, *73*, 254.
[20] X. Zhang, M. D. Do, P. Casey, A. Sulistio, G. G. Qiao, L. Lundin, P. Lillford, S. Kosaraju, *J. Agric. Food Chem.* **2010**, *58*, 6809.
[21] S. Afewerki, A. Sheikhi, S. Kannan, S. Ahadian, A. Khademhosseini, *Bioeng. Transl. Med.* **2019**, *4*, 96.
[22] E. Tavassoli-Kafrani, S. A. H. Goli, M. Fathi, *Int. J. Biol. Macromol.* **2017**, *103*, 1062.
[23] W. E. Hennink, C. F. Van Nostrum, *Adv. Drug Delivery Rev.* **2002**, *54*, 13.
[24] W. Hu, Z. Wang, Y. Xiao, S. Zhang, J. Wang, *Biomater. Sci.* **2019**, *7*, 843.
[25] Y. N. Chen, C. Jiao, Y. Zhao, J. Zhang, H. Wang, *ACS Omega* **2018**, *3*, 11788.
[26] L. Y. Zheng, J. M. Shi, Y. H. Chi, *Macromol. Chem. Phys.* **2018**, *219*, 1.
[27] N. Ninan, A. Forget, V. P. Shastri, N. H. Voelcker, A. Blencowe, *ACS Appl. Mater. Interfaces* **2016**, *8*, 28511.
[28] M. Shin, J. H. Ryu, J. P. Park, K. Kim, J. W. Yang, H. Lee, *Adv. Funct. Mater.* **2015**, *25*, 1270.
[29] I. Gülçin, Z. Huyut, M. Elmastaş, H. Y. Aboul-Enein, *Arabian J. Chem.* **2010**, *3*, 43.
[30] N. Li, X. Yang, W. Liu, G. Xi, M. Wang, B. Liang, Z. Ma, Y. Feng, H. Chen, C. Shi, *Macromol. Biosci.* **2018**, *18*, 1.
[31] V. L. Savic, V. D. Nikolic, I. A. Arsic, L. P. Stanojevic, S. J. Najman, S. Stojanovic, I. I. Mladenovic-Ranisavljevic, *Phytother. Res.* **2015**, *29*, 1117.
[32] G. O. Igile, G. A. Essiet, F. E. Uboh, E. E. Edet, *Int. J. Curr. Microbiol. Appl. Sci.* **2014**, *3*, 552.
[33] A. S. Durmus, M. Yaman, H. N. Can, *Vet. Med. (Praha).* **2012**, *57*, 287.
[34] M. Hasany, A. Thakur, N. Taebnia, F. B. Kadumudi, M. A. Shahbazi, M. K. Pierchala, S. Mohanty, G. Orive, T. L. Andresen, C. B. Foldager, S. Yaghmaei, A. Arpanaei, A. K. Gaharwar, M. Mehrali, A. Dolatshahi-Pirouz, *ACS Appl. Mater. Interfaces* **2018**, *10*, 34924.
[35] M. C. Catoira, L. Fusaro, D. Di Francesco, M. Ramella, F. Boccafoschi, *J. Mater. Sci. Mater. Med.* **2019**, *30*, 115.
[36] J. Guo, W. Sun, J. P. Kim, X. Lu, Q. Li, M. Lin, O. Mrowczynski, E. B. Rizk, J. Cheng, G. Qian, J. Yang, *Acta Biomater.* **2018**, *72*, 35.
[37] R. M. H. Raja Nhari, Y. Che Man, A. Ismail, N. Anuar, *Int. Food Res. J.* **2011**, *817*, 813.
[38] H. Liang, Y. Pei, J. Li, W. Xiong, Y. He, S. Liu, Y. Li, B. Li, *RSC Adv.* **2016**, *6*, 31374.
[39] H. G. Nam, M. G. Nam, P. J. Yoo, J. H. Kim, *Soft Matter* **2019**, *15*, 785.
[40] K. Park, H. Jeong, J. Tanum, J. chan Yoo, J. Hong, *Sci. Rep.* **2019**, *9*, 8308.
[41] E. E. Leonhardt, N. Kang, M. A. Hamad, K. L. Wooley, M. Elsabahy, *Nat. Commun.* **2019**, *10*, 2307.
[42] C. M. Madl, L. M. Katz, S. C. Heilshorn, *ACS Macro Lett.* **2018**, *7*, 1302.
[43] M. Mir, M. N. Ali, A. Barakullah, A. Gulzar, M. Arshad, S. Fatima, M. Asad, *Biomater.* **2018**, *7*, 1.
[44] X. Song, C. Zhu, D. Fan, Y. Mi, X. Li, R. Z. Fu, Z. Duan, Y. Wang, R. R. Feng, *Polymers (Basel)* **2017**, *9*, 1.
[45] N. Annabi, J. W. Nichol, X. Zhong, C. Ji, S. Koshy, A. Khademhosseini, F. Dehghani, *Tissue Eng., Part B* **2010**, *16*, 371.
[46] S. Sornkamnerd, M. K. Okajima, T. Kaneko, *ACS Omega* **2017**, *2*, 5304.
[47] S. Afzal, S. Khan, N. M. Ranjha, A. Jalil, A. Riaz, M. S. Haider, S. Sarwar, F. Saher, F. Naeem, *Turkish J. Pharm. Sci.* **2018**, *15*, 63.
[48] N. Annabi, S. M. Mithieux, E. A. Boughton, A. J. Ruys, A. S. Weiss, F. Dehghani, *Biomaterials* **2009**, *30*, 4550.
[49] N. Annabi, S. M. Mithieux, A. S. Weiss, F. Dehghani, *Biomaterials* **2009**, *30*, 1.
[50] J. Qu, X. Zhao, P. X. Ma, B. Guo, *Acta Biomater.* **2017**, *58*, 168.
[51] B. Xu, C. Sung, B. Han, *Crystals* **2011**, *1*, 128.
[52] I. S. Jahit, N. N. M. Nazmi, M. I. N. Isa, N. M. Sarbon, *Int. Food Res. J.* **2016**, *23*, 1068.
[53] N. Sahiner, S. Sagbas, M. Sahiner, S. Demirci, *Polym. Degrad. Stab.* **2016**, *133*, 152.
[54] K. H. Hong, *Fibers Polym.* **2016**, *17*, 1963.
[55] Z. Xia, A. Singh, W. Kiratitanavit, R. Mosurkal, J. Kumar, R. Nagarajan, *Thermochim. Acta* **2015**, *605*, 77.
[56] G. Svetlichny, I. C. Külkamp-guerreiro, D. F. D. Lana, M. D. Bianchin, A. R. Pohlmann, A. M. Fuentefria, S. S. Guterres, *J. Drug Delivery Sci. Technol.* **2017**, *40*, 59.
[57] J. S. Chin, L. Madden, S. Y. Chew, D. L. Becker, *Adv. Drug Delivery Rev.* **2019**, *149-150*, 2.
[58] J. Qu, X. Zhao, Y. Liang, T. Zhang, P. X. Ma, B. Guo, *Biomaterials* **2018**, *183*, 185.
[59] T. O. Jimoh, T. Ogunmoyole, E. A. Aladejana, I. J. Kade, *Int. J. Ethnopharmacology* **2016**, *2*, 14.
[60] Z. Selamoglu, C. Dusgun, H. Akgul, M. F. Gulhan, *Iran. J. Pharm. Res.* **2017**, *16*, 92.
[61] Z. Fan, B. Liu, J. Wang, S. Zhang, Q. Lin, P. Gong, L. Ma, S. Yang, *Adv. Funct. Mater.* **2014**, *24*, 3933.
[62] P. M. G. Filius, I. C. Gyssens, *Am. J. Clin. Dermatol.* **2002**, *3*, 1.
[63] M. Mehrali, A. Thakur, F. B. Kadumudi, M. K. Pierchala, J. A. V. Cordova, M. A. Shahbazi, M. Mehrali, C. P. Pennisi, G. Orive, A. K. Gaharwar, A. Dolatshahi-Pirouz, *ACS Appl. Mater. Interfaces* **2019**, *11*, 12283.
[64] H. Maleki, M. A. Shahbazi, S. Montes, S. H. Hosseini, M. R. Eskandari, S. Zaunschirm, T. Verwanger, S. Mathur, B. Milow, B. Krammer, N. Hüsing, *ACS Appl. Mater. Interfaces* **2019**, *11*, 17256.
[65] Z. Li, T. Qu, C. Ding, C. Ma, H. Sun, S. Li, X. Liu, *Acta Biomater.* **2015**, *13*, 88.
[66] M. Shahbazi, P. V. Almeida, A. Correia, B. Herranz-blanco, N. Shrestha, E. Mäkilä, J. Salonen, J. Hirvonen, H. A. Santos, *J. Controlled Release* **2017**, *249*, 111.
[67] Y. Hu, Z. Zhang, Y. Li, X. Ding, D. Li, C. Shen, F. J. Xu, *Macromol. Rapid Commun.* **2018**, *39*, 1800069.
[68] C. Li, C. Mu, W. Lin, T. Ngai, *ACS Appl. Mater. Interfaces* **2015**, *7*, 18732.
[69] Y. Hong, F. Zhou, Y. Hua, X. Zhang, C. Ni, D. Pan, Y. Zhang, D. Jiang, L. Yang, Q. Lin, Y. Zou, D. Yu, D. E. Arnot, X. Zou, L. Zhu, S. Zhang, H. Ouyang, *Nat. Commun.* **2019**, *10*, 2060.
[70] Z. K. Kuo, P. L. Lai, E. K. W. Toh, C. H. Weng, H. W. Tseng, P. Z. Chang, C. C. Chen, C. M. Cheng, *Sci. Rep.* **2016**, *6*, 32884.
[71] Y. Hou, N. Carrim, Y. Wang, R. C. Gallant, A. Marshall, H. Ni, *J. Biomed. Res.* **2015**, *29*, 437.
[72] A. Mani, R. Anarthe, P. Kale, S. Maniyar, S. Anuraga, *Galore Int. J. Health Sci. Res.* **2018**, *3*, 40.
[73] J. Yeo, J. Lee, S. Yoon, W. J. Kim, *Biomater. Sci.* **2020**, *8*, 1148.
[74] P. Orlowski, M. Zmigrodzka, E. Tomaszewska, K. Ranoszek-Soliwoda, M. Czupryn, M. Antos-Bielska, J. Szemraj, G. Celichowski, J. Grobelny, M. Krzyzowska, *Int. J. Nanomed.* **2018**, *13*, 991.
[75] Y. Zhou, L. Gao, J. Peng, M. Xing, Y. Han, X. Wang, Y. Xu, J. Chang, *Adv. Healthcare Mater.* **2018**, *7*, 1.
[76] D. Gan, T. Xu, W. Xing, M. Wang, J. Fang, K. Wang, X. Ge, C. W. Chan, F. Ren, H. Tan, X. Lu, *J. Mater. Chem. B* **2019**, *7*, 1716.